The quark–gluon string model: soft and semihard hadronic processes*)

G. I. Lykasov and G. H. Arakelyan**)
Joint Institute for Nuclear Research, Dubna

M. N. Sergeenko
Institute of Physics, Belarus Academy of Sciences, Minsk, Belarus

Fiz. Élem. Chastits At. Yadra **30**, 817–869 (July–August 1999)

The basic principles of the quark–gluon string model, a perturbative QCD approach to describing hadronic processes, are presented. The relation between the s-channel topological $1/N$ expansion of the hadron–hadron scattering amplitude and the t-channel expansion in Regge poles is demonstrated, where N is the number of quark flavors or colors. This approach is used to analyze soft hadronic processes. The attempts to extend the region of applicability of this model to describe the inclusive spectra of resonances and also semihard hadronic processes are briefly reviewed. In particular, a new modification of the model in which Pomeron exchange is treated as the exchange of two nonperturbative gluons with dynamically generated mass is discussed. Soft and semihard processes, and also charmed-particle production in hadron collisions, are analyzed in this version of the model. The advantages and defects of this approach compared to other perturbative QCD models are discussed. © *1999 American Institute of Physics.* [S1063-7796(99)00104-7]

INTRODUCTION

Deep-inelastic particle interactions play a decisive role in the modern theory of fundamental interactions. Whereas lepton–hadron collisions are used to study the quark distribution in hadrons, e^+e^- collisions are used to study the rules of quark hadronization. Hadron–hadron processes at large momentum transfers allow study of the nature of the strong interactions of quarks with various flavors such as color quantum–gluon exchange.

At present there is no unified approach for studying hadron–hadron interactions. This is because hadron interactions are extremely diverse in their properties, both in different energy ranges and in different kinematical regions. The problem is that we are dealing with a nonstatistical system, and any predictions about the behavior of such a system strongly depend on its spacetime evolution.

Many regularities of hadron production in hadron–hadron interactions can be explained quantitatively by using perturbative quantum chromodynamics (QCD), which has had considerable success in describing elementary colored quark and gluon interaction processes under the conditions of asymptotic freedom. Here the leading-log approximation is used, the simple semiclassical form of which is formulated as the Altarelli–Parisi equation.[1] However, the hadron is a very complicated object, continually changing its configuration, both in the number of $q\bar{q}$ pairs which appear and disappear, and in the number of gluons. It is extremely difficult to take into account all the elementary processes in the hadron. Moreover, at high energies the great majority of hadron interactions are soft processes. Perturbative QCD is of very limited use for describing such processes; suffice it to recall the well known difficulties associated with quark confinement, which originate in strong nonperturbative effects.

One of the most popular models of quark confinement is the model of color tubes which can begin and end only on quarks and antiquarks or diquarks. Each such tube is treated as a real physical object having finite energy per unit length. Such a picture ensures linear growth of the interquark interaction potential.[2]

In non-Abelian gauge theories of the strong interaction, confinement is manifested most clearly within the formulation of the theory on a space-time lattice proposed by Wilson.[3] It is remarkable that on the lattice in the strong-coupling limit, confinement is obtained automatically and the theory leads to a picture of interacting quarks located at the ends of strings with finite energy per unit length. Recent studies and lattice calculations have been performed to demonstrate that this phenomenon is preserved in the continuum limit.[4]

At present, an approach to describing hadron interactions is widely used which admits a simple parametrization of the space-time evolution of a quark-gluon system in local equilibrium which contains only longitudinal variables. In this approach, in the c.m. frame of the reaction the fronts of the colliding hadrons move at the speed of light, while an interpolation between these limits is used in the intermediate region. This picture is a rather crude approximation. Obviously, hadrons are broken apart in the interaction process, and instead it is necessary to deal with quark–gluon degrees of freedom rather than hadron ones. In general, the quark–gluon system is a nonequilibrium system: it admits representation by independent strings which are strongly nonequilibrium systems.

Soft interactions cannot be calculated by using QCD. However, it is often forgotten that there exist very successful phenomenological approaches based on the Regge theory (see Ref. 5) for describing hadron–hadron, hadron–nucleus, and nucleus–nucleus interactions in the limit of very high

energies. Such models are fully relativistic quantum theories, and certain features of them can be reproduced in QCD by studying ladder graphs.

Therefore, in high-energy hadron physics there is an approach just as fundamental as QCD itself: the Reggeon theory. There are several fairly well developed models based on this theory: the quark–gluon string model,[6] the dual parton model,[7] and the VENUS model.[5] All these models have proved successful at describing the experimental data, and they are now viewed as the most realistic approach to describing hadron–hadron and hadron–nucleus interactions at high energies. They are more than a simple extrapolation of known physics, as often claimed, because in principle rescattering is included. Most of these models (for example, the dual parton model and the VENUS model) take into account semihard scattering and are capable of reproducing the data up to LHC energies. All these models are identical regarding elastic scattering and the weights of certain inelastic processes; however, the inelastic processes themselves are defined differently.

The need for an adequate (taking into account the experimental conditions) comparison of the large amount of experimental data with the theoretical results has led to the creation of numerous models and programs which generate hadronic and nuclear collisions.[8–11] They are based on the achievements of the standard theory of strong and electroweak interactions and various phenomenological approaches. All the models of hadron–hadron interactions existing at present and the known generating programs can be divided into three groups: models based on the Gribov–Regge theory (the quark–gluon string model, the dual parton model, and the VENUS model), models based on classical string theory (FRITIOF, SRM, ATTILA, SPM), and models based on perturbative QCD (ISAJET, PYTHIA, EUROJET, COJETS/WIZJET, FIELDAJET, HIJING, PCM).[5] Among the generating programs, the ISAJET program[8] and the programs from Lund University, in particular, PYTHIA[9] and FRITIOF,[10] are especially widely known.

Monte-Carlo versions of the quark–gluon string model are under intensive development at present (see Ref. 11 and references therein). These programs attempt to describe the entire range of momentum transfers, from hard quark and gluon scattering to hadron production and decay, which explains why they are so popular.

In the course of fairly long studies, it has become clear that the main problem in the theory of multiple production processes amounts to describing their virtual phase, the spatial dimensions of which exceed the nucleon dimensions and grow with the energy of the colliding particles. The fact that the transformation of virtual particles into real ones occurs at distances of the order of the nuclear size allows the nuclear interaction to be used as a tool for studying the space-time picture of hadronization in particle multiple production processes. In the present review we shall not consider hadron–nucleus interactions, since they represent a separate and quite significant topic of study.

One of the most important and least studied problems in hadron physics is the hadroproduction of particles containing heavy quarks. Realistic estimates of the cross sections for producing heavy quarks in hadron collisions are also needed for planning experiments at existing and future accelerators. The enormous expenses involved in building accelerators and detectors require careful predictions of the experimental situation. Such estimates are usually made on the basis of the parton model within perturbative QCD. However, there are experimental results which contradict the parton model, in which it is impossible to obtain a high yield of charmed particles in K beams compared to π beams.[12] Moreover, parton models systematically underestimate the c- and b-quark production cross sections at relatively low transverse momenta.[13]

The transition of heavy quarks into hadrons is described by various models. In Ref. 12 this is done using the recombination model,[14–16] which takes into account the interaction of newly created heavy Q quarks with quarks from the initial hadrons. This inclusion of the interaction with valence quarks makes it possible to describe the production of the leading component of charmed particles. In this model the recombination function is expressed in terms of the intercept $\alpha_i(0)$ of the leading Regge trajectory associated with the quark q_i. Another phenomenological model[17] has been used to estimate the yield of charmed particles in the Regge approach and to obtain a fairly accurate description of D- and B-meson production using fragmentation functions, which are also expressed in terms of intercepts of the leading Regge trajectories.

A good description of various characteristics of heavy-quark hadroproduction processes can be obtained by using the approach based on the topological $1/N_f$ expansion of the amplitudes in QCD[18–21] and the closely related string and colored-tube models,[22–24] i.e., within the quark–gluon string model.

The main components of the quark–gluon string model are the quark structure functions and the functions describing quark fragmentation into hadrons. These are expressed in terms of intercepts of the trajectories of Regge poles. The largest uncertainty in the calculations of the cross sections for the yields of heavy flavors in the quark–gluon string model is mainly due to the absence of any reliable information about the behavior of the Regge trajectories of heavy $Q\bar{Q}$ quarkonia. Assuming linearity of the $Q\bar{Q}$ trajectories, the intercepts turn out to be low, $\alpha_\psi(0) \simeq -2.2$ and $\alpha_\Upsilon(0) \simeq -16$, and so the contribution of the peripheral mechanism falls off very rapidly with increasing quark mass. Accordingly, the determination of the behavior of the Regge $Q\bar{Q}$ trajectories in the region $0 \leqslant t \leqslant m^2_{Q\bar{Q}}$ and estimation of the intercepts $\alpha_{Q\bar{Q}}(0)$ of the trajectories become especially important.

The quark–gluon string model has been used successfully to describe hadron production processes integrated over the transverse momentum of the created particle and containing not only light u, d, and s quarks. However, it allows the explanation of many characteristic features of the hadroproduction of charmed particles (see Refs. 25 and 26, and also Refs. 27–36). The $1/N_f$ expansion and the model of Reggeized one-pion exchange were used in Ref. 37 to calculate the spectra of Λ_c baryons in pp collisions.

In this review we study modifications of the quark–gluon string model taking into account the dependence of the spectra on the spin of the created particle, namely, the production of resonance states,[32,35,36] and also the dependence of the particle distributions in the transverse momentum of the created particle taking into account the transverse motion of the quarks in the colliding hadrons.[38–45]

In Sec. 1 we briefly describe the main principles of the $1/N$ expansion in QCD and its relation to the Regge theory. We review the studies devoted to the construction of the quark–gluon string model on the basis of this relation. We present a scheme for obtaining the Regge asymptote of the quark distribution functions in the colliding hadrons and the functions describing fragmentation into the produced hadrons. We discuss the features of the interaction of objects with structure compared to the scattering of point particles and the resulting difficulties in describing hadronic processes. A brief characterization of soft hadronic processes is given, and several models of peripheral hadron interactions are studied.

In Sec. 2 we use the quark–gluon string model to analyze the production of boson resonances containing light u-, d-, and s-quarks.[32] Using the model based on the Reggeon–photon analogy, we obtain equations relating the spectra of mesons with higher spins to the spectra of vector (ρ, K^*) and pseudoscalar (π, K) mesons.

Section 3 is devoted to a modification of the quark–gluon string model to describe the hadroproduction of particles with open charm taking into account the contributions from decays of the corresponding S-wave resonances.[35,36]

Section 4 is devoted to a new approach within the quark–gluon string model for describing soft and semihard hadronic processes based on the two-gluon model of the Pomeron.[44,45] In the proposed model the Pomeron is treated as the exchange of two gluons with dynamically generated mass, i.e., a cutoff parameter in $k_\perp$ which vanishes logarithmically at large $k_\perp$ is introduced into the gluon propagator. The proposed version of the quark–gluon string model is used to estimate quantitatively the cross sections for the production of π and D mesons in pp interactions at various initial energies.[44,45] Comparing the calculations for two values of the intercept of the Regge Ψ trajectory, $\alpha_\Psi(0)\simeq 0$ and $\alpha_\Psi(0)=-2.2$, with the experimental data at energy $\sqrt{s}=27.4\,\text{GeV}$, we see that a good description of the spectra both in the Feynman variable x_F and in the transverse momentum $p_\perp$ is obtained for incercept of the Regge Ψ trajectory near zero, $\alpha_\Psi(0)\simeq 0$.

In the Conclusion we briefly state the main results of this study.

1. THE TOPOLOGICAL 1/N EXPANSION AND ITS RELATION TO THE REGGE THEORY

The difficulties associated with the increase of the QCD coupling constant $\alpha_s(Q^2)$ in soft processes have led to the development of alternative approaches to calculating hadronic interactions. The small parameters in QCD can be taken to be $1/N_f$ and $1/N_c$, where N_f is the number of quark flavors $(u,d,s,\ldots)$ and N_c is the number of colors.[18,19] The case close to reality occurs when the ratio N_f/N_c is fixed $(N_f/N_c\propto 1)$ and the expansion is made in $1/N_f$ or $1/N_c$. This approach is called dual topological unitarization,[20,21] because it was proposed independently of QCD for taking into account the unitarity condition within the dual approach. Its connection to QCD was established later.[20]

In processes with small momentum transfers, only light u, d, and s quarks effectively participate, and the number N_f is close to 3, i.e., the expansion parameter is about 1/3. However, the expansion for amplitudes with definite quantum numbers in the t channel is actually made in $1/N_f^2\simeq 0.1$.

In describing multiple production processes, this approach allows a correspondence to be established between the Feynman diagrams of the reaction $a+b\to c+X$ and definite geometrical objects: planar graphs, cylindrical graphs, and graphs with handles and more complicated topologies. Summation over all the types of graph possible in each case allows the amplitudes of soft processes to be obtained as series in $1/N$.

1.1. The topological 1/N expansion in QCD

The approach proposed by 't Hooft[18] uses perturbation theory, however, not in the QCD constant α_s, but in $1/N_c$, where N_c is the number of colors. Here it is assumed that $\alpha_s\cdot N_c=\text{const}$, and the number of flavors N_f is fixed. The QCD Lagrangian is written in a form which can be clearly illustrated as follows. A gluon is treated as a quark–antiquark system, i.e., it is represented as two oppositely directed quark lines. A quark is also represented as two lines (the solid and the dashed lines in Fig. 1a) in the same direction, one of which corresponds to definite color, and the other to definite flavor. Using these rules, the Feynman graphs can then also be depicted differently.

Graphs of the planar and nonplanar type are distinguished. The first include graphs like that shown in Fig. 1a with external gluon lines. For such graphs, all lines can be moved around, without self-intersections, on the plane inside the contour bounded by the quark lines determining the graph boundary. To make this clear, in Fig. 1b we show the equivalent ordinary Feynman graph of QCD, where the wavy lines depict gluons, and the solid lines quarks and antiquarks. The nth-order graph, G_n, where n is the number of external legs or external gluon lines leaving the graph (in Fig. 1, $n=4$) is proportional to the following expression:[3]

$$G_n\propto(g^2)^{2h-2+b}(g^2N_c)^{l_c}(g^2N_f^f)^{l_f}, \tag{1}$$

where we have introduced the following notation: g is the coupling constant, N_c and N_f are the numbers of colors and flavors, respectively, l_c and l_f are the numbers of color and flavor loops, h is the number of handles characterizing the degree of nonplanarity of the graph, and b is the number of boundaries.

In the 't Hooft approach[18] it is assumed that g^2N_c and N_f are fixed constants. A stronger assumption was made in the studies by Veneziano:[19,20] g^2N_c and g^2N_f are fixed. Then in the Veneziano approach

$$G_n\propto(g^2)^{2h+b}\propto\left(\frac{1}{N_c}\right)^{2h+b}\propto\left(\frac{1}{N_f}\right)^{2h+b} \tag{2}$$

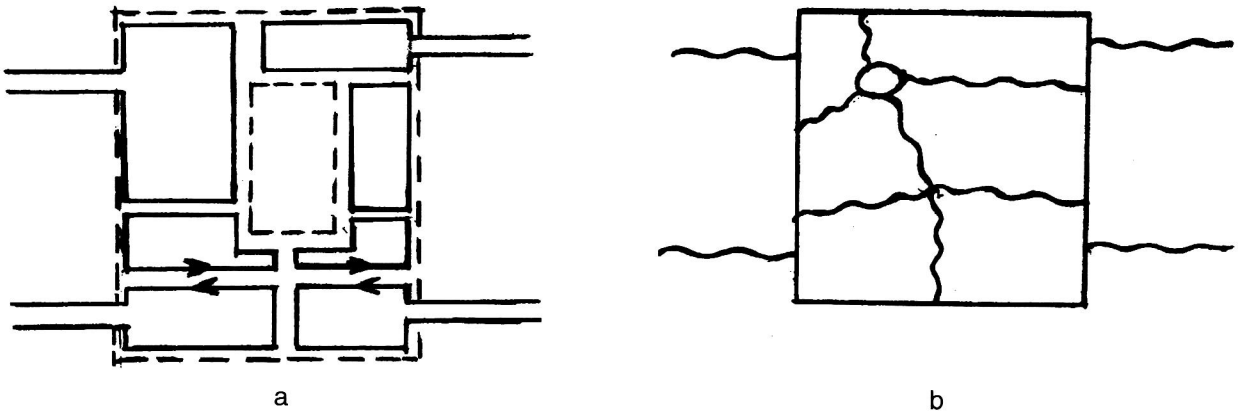

FIG. 1. (a) Planar graph with external legs; (b) the equivalent Feynman graph.

In the topological Veneziano expansion the graphs are classified according to the numbers of handles and boundaries. To obtain, for example, the amplitude of the binary process ($n=4$; see Fig. 2), it is necessary to sum over all h and b, i.e., over the contributions corresponding to different topologies: planar, cylindrical, and so on. We note that the requirement $g^2N_f=\text{const}$ (of order 1) makes the order of the graph n constant, if the quark–antiquark loop is included in it. The main contribution to the topological expansion of the amplitude given above will come, according to Ref. 18, from graphs with $h=0$ and $b=1$, i.e., graphs of the planar type without handles and with a single boundary. Examples of such graphs are given in Fig. 2a for meson–meson scattering. Cutting this graph in the s channel also gives a planar graph for the amplitude of particle multiple production, as shown in Fig. 2b (here and below, to simplify the graphs, the internal quark and gluon lines are not shown, in contrast to Fig. 2a). The amplitudes of such binary processes behave as

$$T_{ab\to cd}^{(h=0,b=1)}\propto\frac{1}{N_f}\propto\frac{1}{N_c}. \tag{3}$$

Graphs of higher topology, when $h=0$ and $b=2$ (called cylindrical graphs, an example of which for elastic scattering is shown in Fig. 3a), behave as follows as a function of N_c or N_f:

$$T_{ab\to ab}^{(h=0,b=2)}\propto\frac{1}{N_f^2}\propto\frac{1}{N_c^2}. \tag{4}$$

Cutting this graph in the s channel corresponds to the cylindrical graph for particle multiple production shown in Fig. 3b. The graphs of next order in topology, the double cylinder with $h=1$ and $b=2$, fall off as $1/N_f^4=1/N_c^4$. The other graphs of the cylindrical type can be represented as multiple cylinders. The latter fall off as $1/N^6$, $1/N^8$,..., because $h=2,3,\ldots$, i.e., each additional cylinder gives a single handle, while the number of boundaries is unchanged: $b=2$.

The dual topological approach proposed in Refs. 18–22 amounts to the following. Planar graphs with $h=0$ and $b=1$ (Fig. 2a) in the s channel are put into correspondence with graphs of one-Reggeon exchange in the t channel. Graphs of the cylindrical type with $h=0$ and $b=2$ (Fig. 3a) correspond to one-Pomeron exchange for elastic scattering $ab\to ab$ in the t channel. Other cylindrical graphs in the s channel with $h=1,2,3,\ldots$ and $b=2$ are put into correspondence with multi-Pomeron exchange graphs for elastic scattering in the t channel. Planar graphs of the cut type (Fig. 2b) thus correspond to multiple production in the collision of mesons a and b consisting of valence quarks and antiquarks. The line determining the left-hand boundary of the cut graph in Fig. 2b corresponds to the annihilation of valence quarks and antiquarks belonging to the colliding hadrons (mesons). The right-hand boundary of that graph depicts a $q\bar{q}$ pair which then fragments into hadrons. Between the left- and right-hand boundaries of that graph is a network of gluon lines and $q\bar{q}$ loops as in Fig. 2a, where they are not shown.

The graph of Fig. 2b cut in the s channel can be interpreted[6] physically as follows. In a collision of two mesons, a quark of one meson annihilates with an antiquark of the other, and the particles of the other $q\bar{q}$ pair interact and then separate in opposite directions (in the c.m. frame of the colliding hadrons). A string is formed between these two quarks in the chromostatic field.[6] It then breaks, resulting in the production of a $q\bar{q}$ pair in the chromodynamic vacuum. The question arises of how to calculate the graph in Fig. 2a, the cut form of which in the s channel is shown in Fig. 2b. The above-mentioned correspondence between the s-channel topological $1/N$ expansion of the amplitude of a binary process and its t-channel expansion in Regge poles (the duality principle) comes to the rescue. At high energies and small momentum transfers, the behavior of the graphs in Fig. 2 in

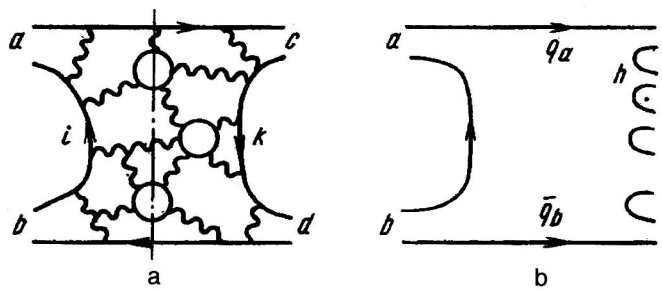

FIG. 2. (a) Planar graph for a binary process; (b) planar graph for a multiple production process.

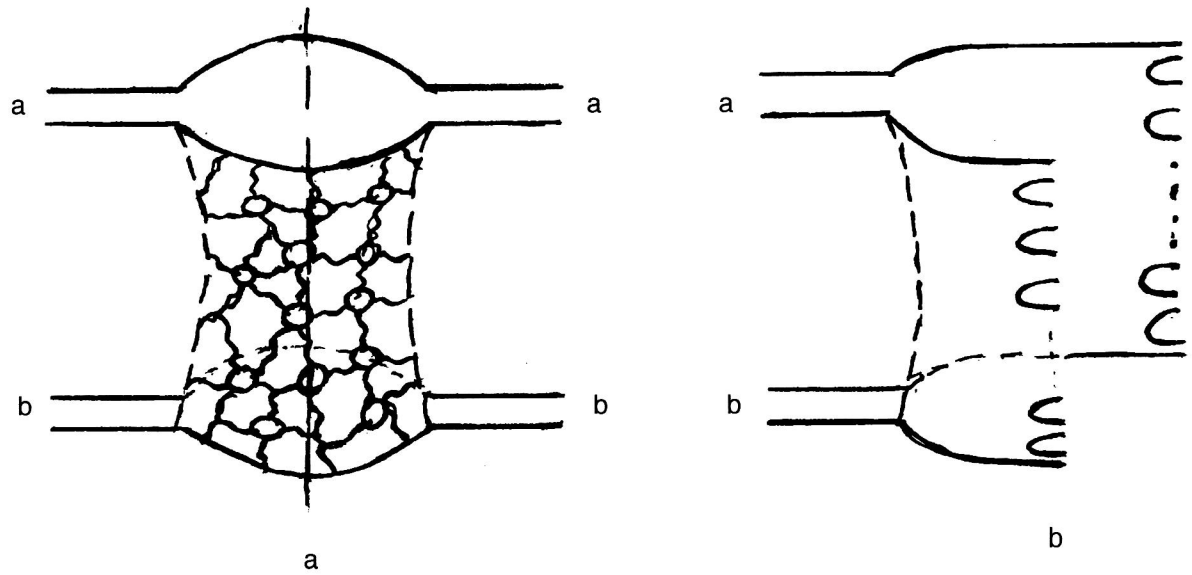

FIG. 3. (a) Cylindrical graph for an elastic process (Pomeron); (b) cylindrical graph for a multiple-production process.

the t channel is determined by the Regge poles with given quantum numbers farthest to the right in the j plane. It is assumed that these poles accurately coincide with the secondary Regge poles observed experimentally $(\rho, A_2, f, \omega, \ldots)$. Multiple hadron production in a collision of particles a and b (Fig. 2b) occurs owing to the multiperipheral mechanism in the t channel.[6] The cross section for this process decreases with increasing s as $(1/s^{1-\alpha_R(0)})$, where the intercept of the Regge trajectory is $\alpha_R(0) \simeq 0.5$. Therefore, planar graphs of the type in Fig. 2 fall off with s as $1/\sqrt{s}$.

The cylindrical graphs of the type shown in Fig. 3 correspond to graphs of Pomeron exchange in the t channel, which in the theory of the supercritical Pomeron do not fall off, but actually grow as s^{Δ}, where $\Delta = \alpha_P(0) - 1 > 0$ (Refs. 6 and 33). The intercept of the supercritical Pomeron is $\alpha_P(0) \simeq 1.27$ (Ref. 6), instead of the usual Pomeron intercept $\alpha_P(0) = 1$. Therefore, the main contribution to hadron multiple production in binary hadronic reactions comes from cylindrical graphs of the type shown in Fig. 3. These graphs can be treated physically like the planar graphs of Fig. 2b: both in the collision of two high-energy protons between a quark of one nucleon and a diquark of the other and, accordingly, the remaining diquark and quark of these nucleons, and in a collision between a color triplet and antitriplet, two color-singlet strings are formed after a color interaction. When the string ends separate, the string breaks, which results in the production of $q\bar{q}$ pairs from the vacuum, which then fragment into hadrons.

The physical treatment of the cylindrical graphs corresponding to multi-Pomeron t-channel exchanges is like that described above, except that instead of two strings, $2n$ color-singlet strings are formed between quarks and diquarks (2 strings) and sea quarks and antiquarks $(2n-2$ strings), where n is the number of Pomeron exchanges in the t channel.

The relation between the s-channel topological $1/N$ expansion of the amplitude of a binary process and its t-channel expansion in Regge poles allows the calculation, starting from the correct Regge asymptote, of the quark distributions in hadrons and their fragmentation functions. It then becomes possible to analyze all soft hadronic processes of hadron multiple production, i.e., processes with small momentum transfers.

The picture of strong hadronic interactions based on the topological expansion allows us to understand many of the properties of strong interactions at high energies.[18–20] However, it is a semiphenomenological theory. The theory of the $1/N$ expansion possesses considerably greater predictive power if the graphs of the topological expansion are compared with a definite space-time picture of quark and gluon interactions, using the color-tube and string model to describe confinement effects.

1.2. The color-tube and quark–gluon string model

The fundamentals of the color-tube fragmentation model are discussed in Ref. 6 and amount to the following. In the region where the quark color field exists, gluon field fluctuations are suppressed, but the vacuum energy prevents the quark color lines of force from penetrating the external medium. This results in a chromodynamic vacuum around the quarks. A hadron is viewed as a bubble in the gluon vacuum, which at the same time signals confinement, since all the lines of force between the quarks are enclosed inside the bubble.[22–24]

A collision of two hadron-bubbles a and b accompanied by valence-quark annihilation is represented as follows in the color-tube model. In order for two quarks q and $\bar{q}$ from different hadrons to annihilate, their relative momenta must be small. Then at high energies of the colliding hadrons rare quark–parton configurations, in which the difference of the quark and antiquark rapidities in the initial hadron (meson) is large, must occur in them. In terms of rapidities this implies

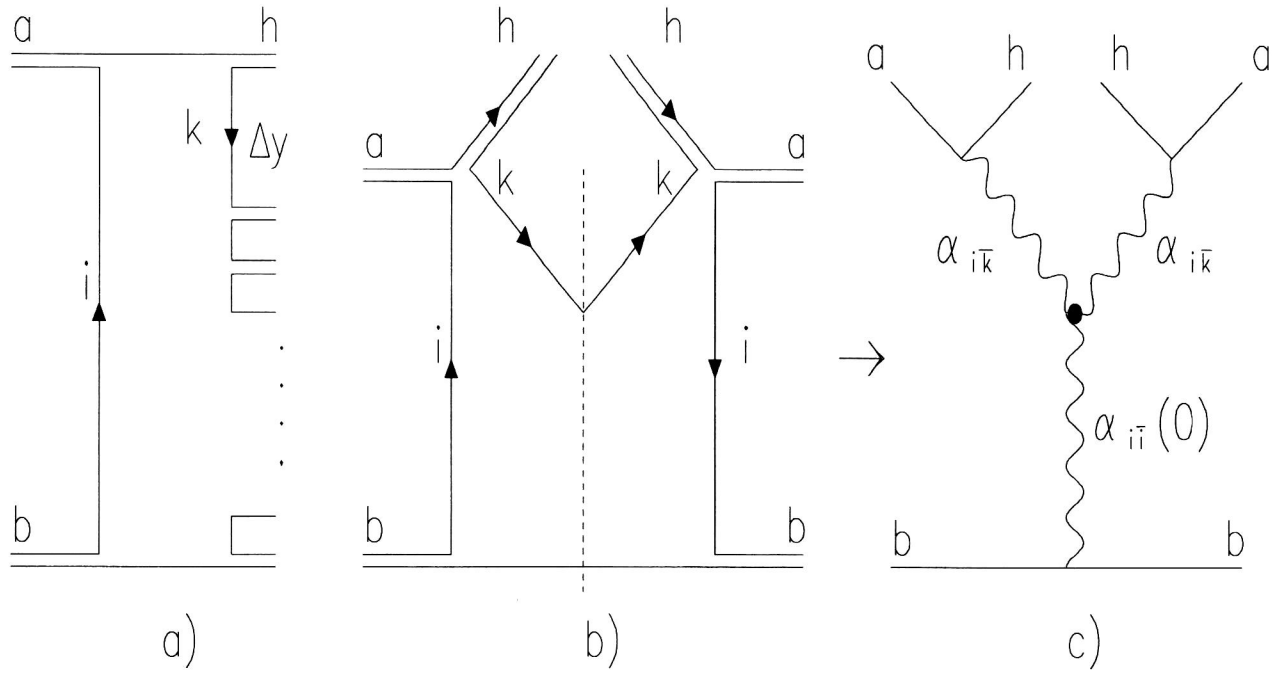

FIG. 4. (a) Planar graph for leading-hadron production; (b) its contribution to the inclusive cross section; (c) three-Reggeon graph corresponding to graph (b) for $x \to 1$.

$$y_q - y_{\bar{q}} \simeq \frac{1}{2} \ln \frac{s}{m_\perp^2}, \tag{5}$$

where $m_\perp^2 = m_q^2 + p_{q\perp}^2$ and $\sqrt{s}$ is the c.m. energy. The complete rapidity interval occupied by the quarks in the colliding hadrons is equal to the total kinematically allowed interval $y_{\max} = \ln(s/m_\perp^2)$.

1.3. The quark distribution in the hadron

In the quark–gluon string model the quark distribution is determined from the correct Regge asymptote of the planar and cylindrical graphs for $x \to 1$ and $x \to 0$, where x is approximately equal to the fraction of the initial hadron momentum due to the quark longitudinal momentum, i.e., $x \sim p_{qz}/p_h$, or, more precisely, the light-cone variable $x = (E_q + p_{qz})/(E_h + p_{hz})$. The Regge asymptote also determines the fragmentation functions, but a few more conditions are imposed. We are actually speaking of the quark distribution at the ends of the $q\bar{q}$ string. Let us first consider the planar graph of Fig. 2b for the binary multiple production process $ab \to hX$ in the c.m. frame of two colliding hadrons a and b, when the particle h is produced as a fast particle, i.e., a process with large x. In this case for $x \to 1$ a large rapidity interval Δy arises between the hadron h and the other particles for $x \to 1$, as shown in Fig. 4a. The corresponding elastic scattering graph is shown in Fig. 4b, where the dashed line shows the cut. The three-Reggeon graph in the t channel corresponding to it is given in Fig. 4c. This problem is discussed in detail in Refs. 6 and 46, and here we shall consider only the basic principles of the construction of the quark distributions in the hadron within the quark–gluon string model.

The creation of a fast particle h in a collision of mesons a and b, corresponding to the planar graph of Fig. 4a, can be treated physically as follows. In a collision of these mesons, which consist of pairs of valence quarks and antiquarks $(q\bar{q})$, the slow antiquark of particle a, denoted by i, undergoes annihilation with the slow quark of particle b. The quark q_a interacts with the antiquark $\bar{q}_b$, after which they separate. A colorless string is formed between them, since q and $\bar{q}$ are a triplet and antitriplet of the color group $SU(3)$. This string is then broken when its ends are far apart, and, according to the Schwinger mechanism,[22] in the chromostatic field quark–antiquark pairs are formed which then undergo fragmentation into hadrons. The production of the particle h can be viewed as the capture of a slow antiquark k (see Fig. 4a), from the chain of quarks and antiquarks formed when the string breaks, by the fast quark q_a. Since the hadron h is fast, it has $x \to 1$, and the rapidity interval Δy between it and the other hadrons is fairly large. The construction of the distribution of the fast quark in the hadron a is equivalent to finding the probability for the other antiquark i to be slowed down in this hadron. We can find this probability from the correspondence between the s-channel planar graph and the t-channel graph with exchange of a Reggeon R (Ref. 6):

$$w_i \sim \sigma_{ab}^{\text{tot}} \sim \operatorname{Im} f_{ab}^{\text{el}}(t=0) \sim \left(\frac{s}{s_0}\right)^{\alpha_R(0)-1} \tag{6}$$

where $\alpha_R(0)$ is the intercept of the Regge trajectory corresponding in this case to exchange of a quark–antiquark pair $q_i\bar{q}_i$ in the s channel, and so it can be denoted by $\alpha_{i\bar{i}}(0)$. Going to the variable x, the fraction of longitudinal momentum of the fast quark q_a, and using the fact that $1 - x \sim 1/s$, this probability can be written as

$$w_i \sim (1-x)^{1-\alpha_{i\bar{i}}(0)} \equiv x_i^{1-\alpha_{i\bar{i}}(0)}, \tag{7}$$

where $x_i = 1-x$ is the fraction of longitudinal momentum of the slow antiquark $\bar{q}_i$ in the hadron a. In a similar manner we can find the probability for the quark (antiquark) k to be slowed down in the production of the hadron h, Fig. 4a, which is equivalent to the probability of finding the fast quark q_a with momentum fraction x at the end of the $q\bar{q}$ string, because $x \simeq 1-x_k$, i.e.,

$$w_k \sim (1-x)^{1-\alpha_{k\bar{k}}(0)} = x_k^{1-\alpha_{k\bar{k}}(0)}, \tag{8}$$

where $\alpha_{k\bar{k}}(0)$ is the intercept of the Regge trajectory corresponding to exchange of quark k and antiquark $\bar{k}$. Passing in (7) and (8) from x_i and x_k to the rapidities y_i, y_k, and $y_{i,k} = \ln(2p_a x_{i,k}/m_{qt})$, where p_a is the momentum of the initial hadron a and m_{qt} is the transverse mass of the valence constituent quark q_a, for w_i and w_k we obtain[6]

$$w_i(\Delta y_i) = C\exp(-\beta_i \Delta y_i); \quad w_k(\Delta y_k) = C\exp(-\beta_k \Delta y_k), \tag{9}$$

where $\Delta y_i = y_a - y_i$, $\Delta y_k = y_a - y_k$, $\beta_i = 1-\alpha_{i\bar{i}}(0)$, and $\beta_k = 1-\alpha_{k\bar{k}}(0)$. Here y_a is the rapidity of the hadron a, y_i and y_k are the rapidities of the quarks i and k (see Fig. 4a), and C is a constant. In Eqs. (6)–(9) we have neglected the quark transverse momenta k_t. When they are included, these expressions involve not the intercepts, but the Regge trajectories depending on k_t^2, i.e., $\alpha_R(-k_t^2)$, which at small k_t^2 can be written as $\alpha_R(-k_t^2) \simeq \alpha_R(0) - k_t^2 \alpha_R'(0)$. Taking this into account and changing over to the space of impact parameters $\mathbf{b}$ in (9), for the Fourier transforms $w_i(\Delta y_i, \mathbf{b})$ and $w_k(\Delta y_k, \mathbf{b})$ we obtain

$$w_i(\Delta y_i, \mathbf{b}) = \frac{C}{4\pi\alpha' \Delta y_i}\exp(-\beta_i \Delta y_i) \times \exp(-\mathbf{b}^2/4\alpha' \Delta y_i), \tag{10}$$

$$w_k(\Delta y_k, \mathbf{b}) = \frac{C}{4\pi\alpha' \Delta y_k}\exp(-\beta_k \Delta y_k) \times \exp(-\mathbf{b}^2/4\alpha' \Delta y_k), \tag{11}$$

where Δy_i, $\Delta y_k \gg 1$, as we are interested in the distribution of the quark q_a at the string end at large x and, accordingly, small x_i and x_k, i.e., for $x \to 1$ (see Fig. 4a). Therefore, Eqs. (9)–(11) give us the probability of slowing down the valence quark i (antiquark $\bar{i}$) in the hadron a (see Fig. 4a) and the probability of creating a slow quark k (antiquark $\bar{k}$) after breaking the string as a function of x (9) or Δy and $\mathbf{b}$. From this it is easy to determine the asymptote of the quark distributions at the ends of the $q\bar{q}$ string. However, here it is necessary to relate the intercept $\alpha_{k\bar{k}}(0)$ to $\alpha_{i\bar{i}}(0)$ and $\alpha_{ik}(0)$, because the latter are known, as will be shown below. The factorization principle in the quark–gluon string model for the amplitude of the binary process $ab \to cd$, shown in Fig. 2, was justified in Ref. 6: the probability of producing various final hadrons c, d depends only on the type of quark k appearing when the string breaks and does not depend on the type of annihilating quark i. Consequently, the imaginary part of the amplitude of the binary process $ab \to cd$ in $\mathbf{b}$ space turns out to be factorized in the s channel:[6]

$$\mathrm{Im} f_{ab\to cd}(\xi, \mathbf{b}) \sim w_{ab}^i(\xi, \mathbf{b}) w_{cd}^k(\xi, \mathbf{b}). \tag{12}$$

Here $\xi = \ln(s/s_0)$ and w_{ab}^i and w_{cd}^k are the same probabilities as w_i and w_k, but for the binary process $ab \to cd$. For elastic scattering $ab \to ab$, using the unitarity condition, we have

$$w_{ik}(\xi, \mathbf{b}) w_{ki}(\xi, \mathbf{b}) \sim w_i(\xi, \mathbf{b}) w_k(\xi, \mathbf{b}), \tag{13}$$

where $w_{ik}(\xi, \mathbf{b})$ is the probability of slowing down both quarks i and k (see Figs. 4a and 4b) with a given impact parameter $\mathbf{b}$. Now, substituting (10) and (11) for w_i and w_k, and also the analogous expression for w_{ik}, into (13), we obtain the following very important relations for the intercepts of the Regge trajectories and their slopes:

$$\alpha_{i\bar{i}}(0) + \alpha_{k\bar{k}}(0) = 2\alpha_{ik}(0), \tag{14}$$

$$(\alpha_{i\bar{i}}'(0))^{-1} + (\alpha_{k\bar{k}}'(0))^{-1} = 2(\alpha_{ik}'(0))^{-1}, \tag{15}$$

where $\alpha_{ik}(0)$ is the intercept of the Regge trajectory corresponding to the exchange of a quark (i) and antiquark ($\bar{k}$) pair in the s channel (see Fig. 4b). From (14) we have

$$-\alpha_{k\bar{k}}(0) = \alpha_{i\bar{i}}(0) - 2\alpha_{ik}(0). \tag{16}$$

Now let us proceed directly to the construction of the asymptote of the quark distributions at the ends of the $q\bar{q}$ string for $x \to 0$ and $x \to 1$. The distribution of the valence quark $q(x)$ in the hadron a for $x \to 0$ can be associated with the probability of finding a slow quark i in a, given by (7):

$$x_i q(x_i) = w_i(x_i) \sim x_i^{1-\alpha_{i\bar{i}}(0)}. \tag{17}$$

From this, for $x \to 0$ we obtain

$$q_a(x) \sim x^{-\alpha_{i\bar{i}}(0)} = x^{-\alpha_R(0)}. \tag{18}$$

As mentioned above, $\alpha_{i\bar{i}}(0) = \alpha_R(0)$ is the intercept of the secondary Reggeon trajectory. The asymptote $q(x)$ for $x \to 1$ is determined by the probability of creating a slow quark k (antiquark $\bar{k}$) after breaking the $q\bar{q}$ string (see Fig. 4b), i.e., according to (8) for $x \to 1$ we have

$$q_a(x) = q_k(1-x) = \frac{w_k(x_k)}{x_k} \sim (1-x)^{-\alpha_{k\bar{k}}(0)}. \tag{19}$$

Or, using (16), Eq. (19) can also be written as

$$q_a(x) = \sim (1-x)^{\alpha_R(0) - 2\alpha_{ik}(0)}. \tag{20}$$

Therefore, the asymptote of the valence-quark distribution in the hadron a, or, more precisely, at the ends of the quark–antiquark string for $x \to 0$ and $x \to 1$, is given by (18) and (19). If the hadron a is taken to be, for example, the π meson, then α_{ik} will correspond to the Reggeon trajectory, i.e., $\alpha_{ik}(0) = \alpha_R(0)$. Then the asymptote of the quark distribution in the π meson for $x \to 0$ and $x \to 1$ will be determined by the following expressions:

For $x \to 0$,

$$q_\pi(x) \sim x^{-\alpha_R(0)} = x^{-1/2}, \tag{21}$$

and for $x \to 1$,

$$q_\pi(x)\sim(1-x)^{-\alpha_R(0)}=(1-x)^{-1/2}. \quad (22)$$

The asymptote of the quark distribution in the nucleon for $x\to 1$ is determined by the probability of slowing down the diquark qq in the nucleon (see Fig. 4a), i.e., according to (7),

$$w_{qq}(x_{qq})\sim x_{qq}^{1-\alpha_{(qq)(\bar{q}\bar{q})}(0)}, \quad (23)$$

where $x_{qq}=1-x$ is the diquark momentum fraction in the nucleon, and $\alpha_{(qq)(\bar{q}\bar{q})}(0)$ is the intercept of the Regge trajectory containing the diquark and antiquark, which satisfies Eq. (14), i.e.,[6]

$$\alpha_{(qq)(\bar{q}\bar{q})}(0)+\alpha_{k\bar{k}}(0)=2\alpha_{3q}(0). \quad (24)$$

Then, using (23), for $x\to 1$ we have

$$q_N(x)=\frac{w_{qq}(x_{qq})}{x_{qq}}=C_1x_{qq}^{-\alpha(qq)(\bar{q}\bar{q})(0)}$$
$$=C_1(1-x)^{\alpha_{k\bar{k}}(0)-2\alpha_{3q}(0)}. \quad (25)$$

In this case $\alpha_{k\bar{k}}(0)=\alpha_R(0)$, and $\alpha_{3q}=\bar{\alpha}_B(0)$ is the averaged intercept of the baryon trajectory.[6] The behavior of $q_N(x)$ for $x\to 0$ is also determined by (21), as for the π meson.

We again note that here we are presenting only the principles of obtaining the Regge asymptote of the quark distributions in the hadron, in particular, in the π meson and the nucleon for $x\to 0$ and $x\to 1$. A detailed discussion of this problem can be found in Ref. 6. If we substitute into (25) the values of the intercepts $\alpha_R(0)=\frac{1}{2}$ and $\bar{\alpha}_B(0)\simeq -0.5$ following from the experimental data, as shown in Ref. 6, then for $x\to 1$ we have

$$q_N(x)\sim(1-x)^{3/2}. \quad (26)$$

The asymptote of the valence-quark distribution in the nucleon for $x\to 0$, in principle, coincides with the analogous distribution observed in deep-inelastic lepton–nucleon scattering. According to (26), for $x\to 1$ it differs fundamentally from the corresponding behavior observed in deep-inelastic scattering.[47] This may be related to the fact that in the quark–gluon string model the quarks are constituent quarks, while in deep-inelastic scattering they are point or current quarks, as in QCD.

1.4. Quark and diquark fragmentation into hadrons

The asymptote of the functions describing quark fragmentation into hadrons for $x\to 1$ is also determined by the three-Reggeon graph in the t channel (Fig. 4c) or its s-channel analog (Fig. 4b). The details of the derivation of this asymptote are given in Ref. 6; here we only briefly explain the principles of how it was obtained.

Let us assume that the leading hadron c, i.e., with momentum fraction $z=p_c/p_a\to 1$, is formed in the process $a+b\to c+X$. Then the inclusive relativistically invariant spectrum of this hadron $f_c\equiv E_c d\sigma/d^3p$ at this z is determined by the three-Reggeon graph in the t channel shown in Fig. 4c. As is well known,[6] this z behavior for $z\to 1$ is written as

$$f_c(z,p_t)\sim g(p_t^2)(1-z)^{\alpha_{i\bar{i}}(0)-2\alpha_{ik}(p_t^2)}, \quad (27)$$

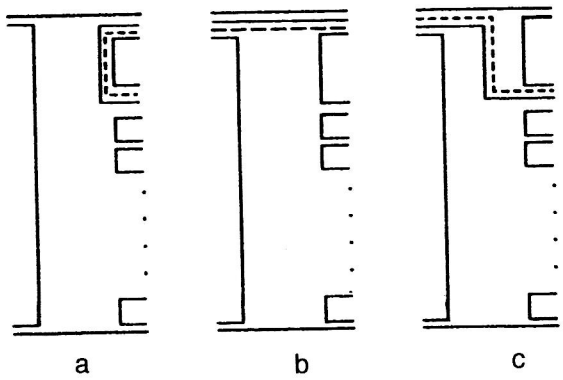

FIG. 5. Planar graphs for baryon production in the quark–gluon string model in the limit $x\to 1$.

where $g(p_t^2)$ is some function depending on the squared transverse momentum of the produced hadron p_t^2. On the other hand, the spectrum (27) can be written as

$$f_c(z,p_t)\equiv D^c_{q_a}(z,p_t^2)z, \quad (28)$$

where $D^c_{q_a}(z,p_t^2)$ is the function describing the fragmentation of the quark q_a into the hadron c. In the limit $z\to 0$ ($y_{q_a}-y_c\gg 1$) the function $f_c(z,p_t^2)$ does not depend on z, i.e., for $z\to 0$

$$D^c_{q_a}(z,p_t^2)\sim\frac{g(p_t^2)}{z}. \quad (29)$$

Comparing (27)–(29), we have

$$D^c_{q_a}(z,p_t^2)=\frac{g(p_t^2)}{z}(1-z)^{\alpha_{i\bar{i}}(0)-2\alpha_{ik}(p_t^2)}. \quad (30)$$

Equation (30) is the general form of the function describing the fragmentation of the quark q_a into the hadron c. For simplicity, let us consider the fragmentation functions integrated over p_t^2. The behavior of $D^c_{q_a}(z)$ for $z\to 1$ can be obtained from (30) by expanding $\alpha_{i\bar{k}}$ in a series in p_t^2, replacing p_t^2 by its average value $\overline{p_t^2}$ and using (14):

$$D^c_{q_a}(z,p_t^2)\sim(1-z)^{-\alpha_{k\bar{k}}(0)+\lambda}, \quad (31)$$

where $\lambda=2\alpha'_{i\bar{k}}\overline{p_t^2}$. Equation (31) is the asymptote of the fragmentation function for $z\to 1$ for the allowed fragmentation, i.e., for the case where the quark q or diquark (qq) forms a part of the hadron c.

Let us consider several examples for $z\to 1$ (Ref. 46):

$$D_u^{\pi^+}(z)=D_{\bar{d}}^{\pi^-}(z)\sim(1-z)^{\alpha_\rho(0)+\lambda}, \quad (32)$$

$$D_u^{K^+}(z)=D_{\bar{u}}^{K^-}(z)\sim(1-z)^{-\alpha_\phi(0)+\lambda}, \quad (33)$$

$$D^p_{ud}(z)=D^n_{ud}(z)\sim(1-z)^{-\alpha_\rho(0)+\lambda}. \quad (34)$$

In the case of the production of baryons by a quark or mesons by a diquark (see the graphs in Fig. 5), the diquark plays the role of the state k, i.e. two quarks and the color node, shown by the dashed line in Fig. 5, introduced in Ref. 48 in describing baryons in QCD. The trajectories $\alpha_{qq(\bar{q}\bar{q})}$ containing a diquark and an antidiquark satisfy (24).

In particular, the intercept of the trajectory $\alpha_{qqq}(0)$ for light (u,d) quarks can be written as

$$\alpha_{ud\bar{u}\bar{d}}(0)=2\alpha_N(0)-\alpha_\rho(0). \tag{35}$$

Using (24), (31), and (35), we can obtain the functions describing the fragmentation of quarks into baryons and diquarks into mesons for $z\to 1$. For example,[46]

$$D_u^p(z)=D_d^n(z)\sim(1-z)^{\alpha_\rho(0)-2\alpha_N(0)+\lambda}, \tag{36}$$

$$D_{ud}^{K^+}(z)\sim D_{uu}^{K^+}(z)\sim(1-z)^{\alpha_\rho(0)-2\alpha_N(0)+\lambda}. \tag{37}$$

These fragmentation functions, and also their asymptote for $z\to 1$ for cases where the hadron c does not contain an initial quark or diquark ("forbidden" fragmentation), are discussed in detail in Ref. 46. The construction of the asymptote of the fragmentation function for forbidden fragmentation amounts to the following. In such cases the hadron c is created not directly in the first $q\bar{q}$ chain, but in subsequent chains in the production of slow $q\bar{q}$ pairs, and so the asymptote of the fragmentation function for $z\to 1$ acquires, as shown in Ref. 46, an additional factor $(1-z)^{1-\alpha_{q\bar{q}}(0)}$ associated with the slowing of each quark. For example,

$$D_u^{\pi^-}(z)\sim(1-z)^{-\alpha_\rho(0)+2(1-\alpha_\rho(0))+\lambda}, \tag{38}$$

$$D_u^{K^-}(z)\sim(1-z)^{-\alpha_\rho(0)+(1-\alpha_\rho(0))+(1-\alpha_\phi(0))+\lambda}. \tag{39}$$

Therefore, the asymptote of the fragmentation function for $z\to 1$ is determined by the intercepts of the secondary Regge trajectories and their derivatives for $p_t^2=0$, the values of which can be taken from the experimental data. We note that this asymptote of the fragmentation function also differs fundamentally from the analogous behavior of the fragmentation function obtained in deep-inelastic scattering or hard hadronic processes, like the quark distributions in the hadron.[47]

2. RESONANCE PRODUCTION IN THE QUARK–GLUON STRING MODEL

A large amount of data has recently appeared on the inclusive hadroproduction of resonances with various quantum numbers. In particular, there are relatively accurate data on the x and $p_\perp$ spectra of secondary mesons, and also some characteristics of the production of resonances with high ($J\geqslant 2$) spin have been measured. The correct description of these data requires more detailed development of the existing soft interaction schemes. One of the most important problems in this area is the inclusion of the spin variables in the quark–parton models used to describe multiple production processes.[10,47,49]

Let us consider the generalization of the quark–gluon string model to the case of the production of boson resonances[32] lying on the leading trajectory of the vector–tensor ($V-T$) group ($\rho,a_2,f,K^*,\ldots$). This approach is based on the Reggeon–photon analogy, which allows the spin J of observed resonances to be taken into account. For this it is necessary to consider the functions $G^J_{q(qq)}(z)$ describing the fragmentation of quarks and diquarks into boson resonances with arbitrary spin J. The functions $G^J_{q(qq)}(z)$ for $z\to 1$ are expressed in terms of the residues of the secondary Regge trajectories corresponding to the contribution of planar graphs in dual topological unitarization. Using the predictions of the quark–gluon string model for the spin structure of the planar graphs,[50] relations between the residues of the leading trajectories of the $V-T$ group were obtained. According to these predictions, the interaction of Reggeons of the $V-T$ group with hadrons has a universal form, analogous to the case of the electromagnetic interaction. The hypothesis that electromagnetic interactions dominate in the planar part of the hadron amplitudes (or the Reggeon–photon analogy), together with the predictions of the Veneziano dual model[51] for the Reggeon–particle vertices, allows the values of $G^J_{q(qq)}(z)$ to be fixed for $z\to 1$. As a result, we obtain a simple expression determining the dependence of the resonance production cross section on the resonance spin J.

The expression for the invariant inclusive hadron spectrum is written in the following form in the quark–gluon string model (see, for example, Refs. 25 and 28):

$$\frac{d\sigma^h}{dy}\equiv x_R\frac{d\sigma^h}{dx}=\int E\frac{d\sigma}{d^3\vec{p}}d^2p_\perp=\sum_n \sigma_n(s)\varphi_n^h(s,x), \tag{40}$$

where y is the rapidity, $x=2p_z/\sqrt{s}$ is the Feynman variable, p_z is the longitudinal momentum of the created hadron, $\sqrt{s}$ is the total energy of the two colliding hadrons in the c.m. frame, σ_n is the cross section for producing an n-Pomeron shower (or $2n$ quark–gluon strings decaying into hadrons),[6,27] $\varphi_n^h(s,y)$ is the hadron distribution in the n-Pomeron shower, $x_R=(x_\perp^2+x^2)^{1/2}$, $x_\perp^2=4(\langle p_\perp^2\rangle+m_h^2)/s$, and m_h and $\langle p_\perp\rangle$ are the secondary-hadron mass and average transverse momentum. The cross sections σ_n for the emission of n Pomeron showers are calculated from the expressions (the quasieikonal model; Ref. 52)

$$\sigma_n=\frac{\sigma_P}{nz}\left(1-e^{-z}\sum_{k=0}^{\infty}\frac{z^k}{k!}\right),\quad n\geqslant 1, \tag{41}$$

$$z=\frac{2C_P\gamma_P}{R_P^2+\alpha_P'\ln(s/s_0)}\left(\frac{s}{s_0}\right)^{\Delta}, \tag{42}$$

$$\sigma_P=8\pi\gamma_P\left(\frac{s}{s_0}\right)^{\Delta}, \tag{43}$$

where σ_P is the Pomeron contribution to the total cross section, $\Delta=\alpha_P(0)-1$ is the excess of the Pomeron intercept above 1 (the supercritical Pomeron), the parameters γ_P and R_P^2 determine the strength of the Pomeron–hadron coupling, and the parameter C_p takes into account the deviation from the eikonal approximation. The values of the remaining parameters will be given below in the calculation of the cross sections for specific reactions. The total hadron interaction cross section in the quark–gluon string model is the sum of the cross sections $\sigma_n(s)$ for creating any number of Pomeron showers:

$$\sigma_{\text{tot}}(s)=\sum_{n=0}^{\infty}\sigma_n(s), \tag{44}$$

$$\sigma_{\text{in}}(s)=\sigma_0^{DD}+\sum_{n=1}^{\infty}\sigma_n(s),\quad \sigma_0^{DD}=(1-1/c)\sigma_0(s), \tag{45}$$

where σ_0^{DD} is the cross section for diffraction dissociation,

$$\varphi_n^{\pi(K)p\to h}(x_F)=f_{\bar{q}}^h(x_+,n)f_q^h(x_-,n)+f_q^h(x_+,n)f_{qq}^h(x_-,n)+2(n-1)f_{\text{sea}}^h(x_+,n)f_{\text{sea}}^h(x_-,n), \tag{46}$$

$$\varphi_n^{pp\to h}(x_F)=f_{qq}^h(x_+,n)f_q^h(x_-,n)+f_q^h(x_+,n)f_{qq}^h(x_-,n)+2(n-1)f_{\text{sea}}^h(x_+,n)f_{\text{sea}}^h(x_-,n), \tag{47}$$

$$x_\pm=\frac{1}{2}\left(\left[\frac{4m_\perp^2}{s}+x_F^2\right]^{1/2}\pm x_F\right). \tag{48}$$

The functions $f_{qq}^h(x_\pm,n)$, $f_q^h(x_\pm,n)$, $f_{\bar{q}}^h(x_\pm,n)$, and $f_{\text{sea}}^h(x_\pm,n)$ appearing in (46) and (47) determine the secondary-particle inclusive spectra and are expressed in terms of convolutions of the momentum distributions $u(x)$ of diquarks and valence and sea quarks (antiquarks) in the colliding hadrons and the functions $G^h(z)$ describing diquark and quark fragmentation into the created hadrons. The contributions from the initial particle and the target proton respectively depend on the variables x_+ and x_-. For the case of pp collisions these convolutions have the form[25]

$$f_{qq}^h(x_\pm,n)=\frac{2}{3}\int_{x_\pm}^1 u_{ud}(x_1,n)G_{ud}^h(x_\pm/x_1)dx_1+\frac{1}{3}\int_{x_\pm}^1 u_{uu}(x_1,n)G_{uu}^h(x_\pm/x_1)dx_1, \tag{49}$$

$$f_q^h(x_\pm,n)=\frac{2}{3}\int_{x_\pm}^1 u_u(x_1,n)G_u^h(x_\pm/x_1)dx_1+\frac{1}{3}\int_{x_\pm}^1 u_d(x_1,n)G_d^h(x_\pm/x_1)dx_1, \tag{50}$$

$$f_{\text{sea}}^h(x_\pm,n)=\frac{1}{2+\delta}\left[\int_{x_\pm}^1 u_{\bar{u}}(x_1,n)\frac{G_{\bar{u}}^h(x_\pm/x_1)+G_u^h(x_\pm/x_1)}{2}dx_1+\int_{x_\pm}^1 u_{\bar{d}}(x_1,n)\frac{G_{\bar{d}}^h(x_\pm/x_1)+G_d^h(x_\pm/x_1)}{2}dx_1+\delta\int_{x_\pm}^1 u_{\bar{s}}(x_1,n)\frac{G_{\bar{s}}^h(x_\pm/x_1)+G_s^h(x_\pm/x_1)}{2}dx_1\right]. \tag{51}$$

The parameter $\delta\sim 0.2$–0.3 determines strange-quark suppression in the sea.

Similarly, for $\pi^- p$ collisions

$$f_q^h(x_+,n)=\int_{x_+}^1 u_d(x_1,n)G_d^h(x_+/x_1)dx_1,$$

$$f_{\bar{q}}^h(x_+,n)=\int_{x_+}^1 u_{\bar{u}}(x_1,n)G_{\bar{u}}^h(x_+/x_1)dx_1. \tag{52}$$

The expressions for the Kp interaction have the same structure as (52).

The properties of the fragmentation functions within the quark–gluon string model were discussed in Sec. 1 above.[6,46] The behavior of the fragmentation functions $G_{q(qq)}^h(z)$ in the two asymptotic limits $z\to 0$ and $z\to 1$ can be determined by their Regge asymptotes:

$$G_{q(qq)}^h(0)=b^h, \tag{53}$$

$$G_{q(qq)}^h(z\to 1)\sim(1-z)^\gamma. \tag{54}$$

Here γ is determined by the intercepts of the corresponding Regge trajectories. For our purposes it is most important to study the constant b^h, which is the value of the function $G_{q(qq)}^h(z)$ for $z\to 0$ and does not depend on the type of initial quark q (diquark qq). The constant b^h is determined by the string fragmentation dynamics, when a $q\bar{q}$ pair is created from the vacuum in the central region of the spectrum. For example, it follows from $SU(3)$ symmetry that $b^{\rho^+}=b^{\rho^-}=b^{\rho^0}=b^\rho$, $b^\omega=b^\rho,\ldots$. These constants cannot be calculated directly in the quark–gluon string model. Below, we shall give estimates for the ratio of these constants obtained using the Reggeon–photon analogy.

The main assumption that we make is that the shape of the x_F spectra of resonances created when the quark–gluon string breaks is independent of the spin J of the observed resonance, i.e., all states lying on the Regge trajectory $\alpha_{ik}(M_J^2)$ have the same type of x dependence for identical initial conditions. With this approximation the functions describing quark (diquark) fragmentation into various resonances of the ρ and K^* families can be expressed in terms of the function for fragmentation into ρ or K^* mesons:[32]

$$G_{q(qq)}^J(x)=R_J G_{q(qq)}^{\rho,K^*}(x), \tag{55}$$

where R_J is independent of the variable x.

The full list of functions describing fragmentation into vector mesons is given in Appendix A. In the parametrization (55) the quantities R_J are expressed in terms of the constants b^J: $R_J=(b^J/b^V)^2$. Analysis of the data on ρ-meson production in πN collisions in the quark–gluon string model[53] gives

$$b^\rho\approx 0.27,\quad b^{K^*}\approx 0.15. \tag{56}$$

Let us now return to the fragmentation functions for high-spin states. The ratios R_J are derived in detail by using the Reggeon–photon analogy in Ref. 32. Here we shall only briefly discuss the main results, for example, for the reaction $\pi N\to JX$. In the three-Reggeon limit we have

$$\frac{d\sigma^J}{dx}(x\to 1)\Big/\frac{d\sigma^V}{dx}(x\to 1)=R_J=(b^J/b^V)^2=\sum_{\lambda=-J}^{J}|g_{0\lambda}^{\pi\alpha_V J}(0)|^2\Big/\sum_{\lambda=-1}^{1}|g_{0\lambda}^{\pi\alpha_V V}(0)|^2, \tag{57}$$

where $g_{0\lambda}^{\pi\alpha_V J}$ are the s-channel helicity residues of the Regge trajectories α_V of the $V-T$ group. Use of the Reggeon–photon analogy allows us to calculate the relations between the residues $g_{0\lambda}^{\pi\alpha_V J}$. Let us discuss this analogy in more de-

tail. The ρ-meson–photon analogy was first proposed by Stodolsky and Sakurai[118] for describing the characteristics of Δ-isobar production in the reactions $\pi p \to \pi\Delta$ and $Kp \to K\Delta$. It was assumed that the spin structure of these processes has an electromagnetic form. Some results supporting this hypothesis were obtained in Refs. 50 and 119. Analysis of the contribution of planar graphs to the total hadron–hadron interaction cross sections showed that the residues of the leading Regge trajectories satisfy relations typical of vector currents.[119] In particular, the interaction of π and K mesons and nucleons with the ρ trajectory is analogous to the isovector component of the electromagnetic current. Similarly, the interactions with the ω and φ trajectories are similar to the nonstrange and strange components of the isovector current, respectively.

The amplitude of the quark–quark interaction was studied by using the multiperipheral mechanism in Ref. 50. This mechanism allows understanding of the location in the j plane of secondary Regge trajectories with various quantum numbers, and also predicts the spin structure of the interaction of these trajectories with quarks. The spin structure describing the interaction of quarks with trajectories of the $V-T$ group has an electromagnetic form:

$$M_{qq}^{V-T} \sim \bar{q}_3 \gamma^\mu q_1 \bar{q}_4 \gamma_\mu q_2 . \tag{58}$$

It seems natural to generalize the Reggeon–photon analogy to the case of arbitrary spin. We assume that the interactions of Reggeons of the $V-T$ group with arbitrary hadrons are determined by the conserved vector current. In the case of the transition $\pi \overset{\alpha_V}{\to} J$, this current has the form

$$j^\mu(\lambda) = iF_J \varepsilon^{\alpha\beta\gamma\mu} \varphi_{\alpha\nu_1\ldots\nu_{J-1}}(k,\lambda) p_\beta k_\gamma q^{\nu_1} \ldots q^{\nu_{J-1}}, \tag{59}$$

where p and k are the 4-momenta of the initial pion and the final resonance, respectively. In (59) $q=k-p$ and $\varphi_{\alpha\nu_1\ldots\nu_{J-1}}(k,\lambda)$ is the wave function of the resonance with spin J and helicity λ. In the infinite-momentum frame $p^{0,3} \to \infty$, and the helicity residue $g_{0\lambda}^{\pi\alpha_V J}(q)$ is related to the current (59) as

$$g_{0\lambda}^{\pi\alpha_V J}(q) e^{-i\varphi\lambda} = j^{0,3}(\lambda)/2p^{0,3}. \tag{60}$$

Using (59) and (60), we find

$$\sum_{\lambda=-J}^{J} |g_{0\lambda}^{\pi\alpha J}(q)|^2 = |F_J|^2 (J+1)!(J-1)! 2^{J-3} p_t^{2(J-1)} \bar{q}_\perp^2/(2J)!. \tag{61}$$

Let us discuss the dependence of F_J on the spin J. For this we consider the decay of a resonance with spin J into a pseudoscalar and a vector, i.e., the on-shell vertex function $J \to \pi V$. Using (59), it is easy to obtain the following expression for the width $\Gamma_{J\to\pi V}$ of the decay $J \to \pi V$:

$$\Gamma_{J\to\pi V} = \frac{p_t}{8\pi M_J^2} \frac{1}{(2J+1)} \sum_{\lambda',\lambda} |j^\mu(k,\lambda)\xi_\mu(q,\lambda')|^2 = \frac{2^J (J+1)!(J-1)!}{8\pi(2J+1)!} |F_J|^2 p_t^{2J+1}. \tag{62}$$

Comparing (62) with the predictions of the resonance-decay model,[120] we find the expression

$$|F_J|^2 = \frac{2^{J-1}}{(J-1)! s_0^{J-1}} |F_V|^2, \tag{63}$$

where $s_0 = (\alpha_V')^{-1}$.

We note that a similar J dependence of F_J follows from the analytic dependence of the Veneziano dual amplitude.[51] Finally, assuming that the ratio $|F_J|^2/|F_V|^2$ is independent of the off-shell corrections, it is easy to obtain the expression for the ratio $R_J(t)$ in (57):

$$R_J(t) = \sum_{\lambda=-J}^{J} |g_{0\lambda}^{\pi\alpha_V J}(q)|^2 \Big/ \sum_{\lambda=-1}^{1} |g_{0\lambda}^{\pi\alpha_V V}(q)|^2 = \frac{(J+1)!}{(2J)!} \left(\frac{4p_t^2}{s_0}\right)^{J-1}. \tag{64}$$

Equations (57) and (64) can be used to express the b^J determining the probability of forming resonances with spin J in terms of the intercept $\alpha_V(0)$ of the trajectory to which the resonance J belongs:

$$R_J \equiv R_J(0) = (b^J/b^V)^2 = \sigma^J/\sigma^V = \frac{(J+1)!}{(2J)!} (J - \alpha_V(0))^{J-1}, \tag{65}$$

where we have used the fact that $J = \alpha_V(0) + \alpha_V' M_J^2$ and $\mu^2 \ll M_J^2$.

It follows from (65) that

$$(b^{f_2})^2 = (b^{a_2})^2 \approx 0.38 (b^\rho)^2,$$
$$(b^{\omega_3})^2 = (b^{\rho_3})^2 \approx 0.21 (b^\rho)^2,$$
$$(b^{f_4})^2 \approx 0.13 (b^\rho)^2. \tag{66}$$

Similarly, for resonances of the K^*-K^{**} family we have

$$(b^{K_2^*})^2 \approx 0.44 (b^{K^*})^2,$$
$$(b^{K_3^*})^2 \approx 0.25 (b^{K^*})^2,$$
$$(b^{K_4^*})^2 \approx 0.16 (b^{K^*})^2. \tag{67}$$

Furthermore, using the model predictions for resonance decay,[119,120] we obtain relations between the probabilities for producing pseudoscalar and vector mesons:

$$(b^\rho/b^\pi)^2 = \langle \vec{k}_\perp^2 \rangle_\pi / 4m_q^2,$$
$$(b^{K^*}/b^K)^2 = \langle \vec{k}_\perp^2 \rangle_K / 4m_q^2, \tag{68}$$

where $m_q = 0.415 \pm 0.015$ GeV is the transverse mass of a constituent quark.[120] Using $\langle \vec{k}_\perp^2 \rangle_\pi \approx 0.12\,\text{GeV}^2$ and $\langle \vec{k}_\perp^2 \rangle_K \approx 0.21\,\text{GeV}^2$, and also the values of b^ρ and b^{K^*} given in (56) (Ref. 53), we find

$$b^\pi \approx 0.65, \quad b^K \approx 0.27. \tag{69}$$

These values are in good agreement with those obtained in Refs. 27 and 29 from analysis of the data on pseudoscalar-meson production.

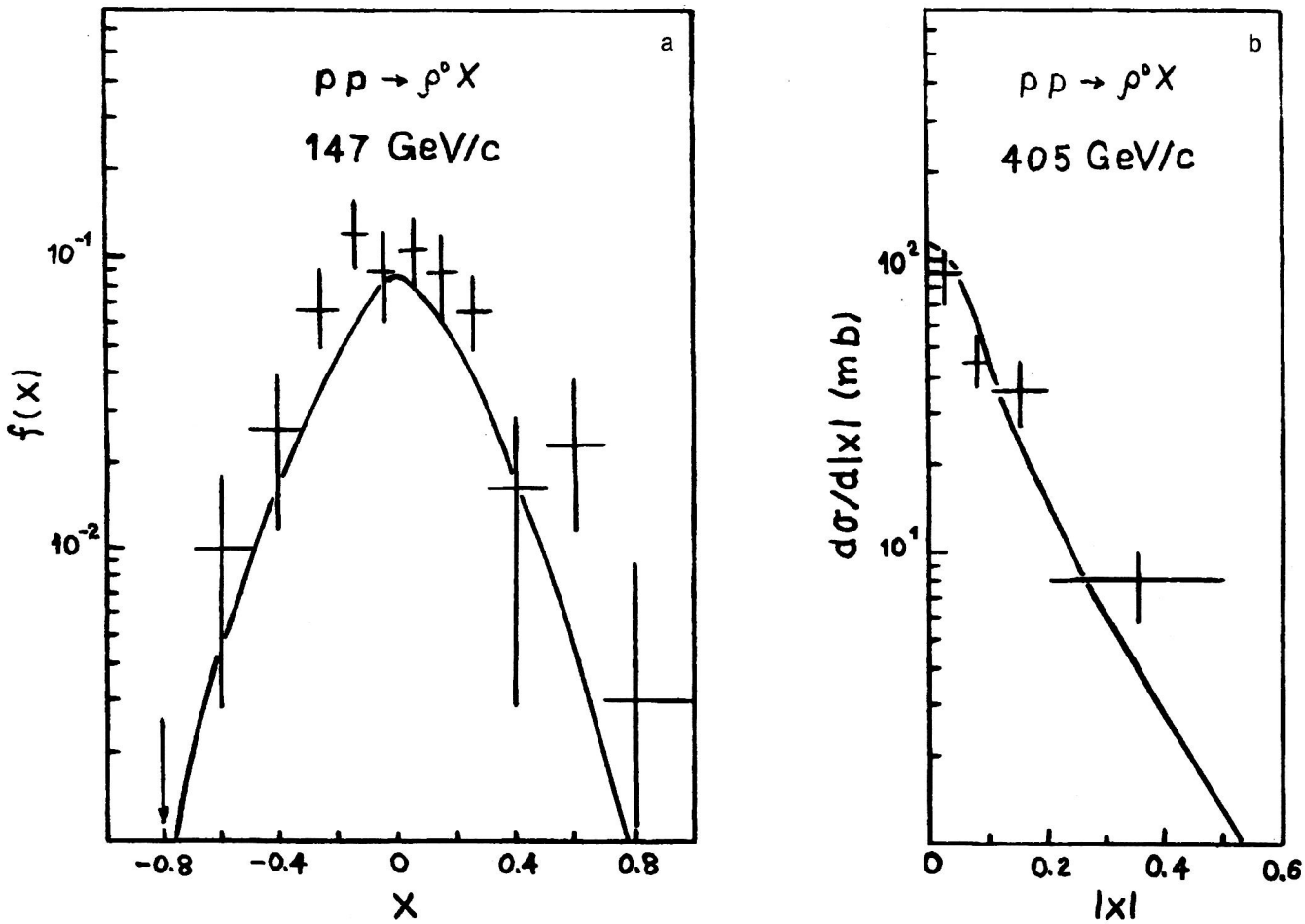

FIG. 6. Inclusive spectra of the ρ^0 meson in pp collisions at $p_L = 147$ GeV/c (Ref. 55) and 405 GeV/c (Ref. 56); $f(x) = (2/\sigma_{in}\sqrt{s}) \int E(d^2\sigma/dx dp_\perp^2)\, dp_\perp^2$.

The experimental data on vector-meson production in πp and pp collisions[54–63] are compared with our predictions in Figs. 6 and 7. We see that the quark–gluon string model gives a good reproduction of the x spectra of vector mesons in a wide range of x at high energies ($p_L \geq 100$ GeV/c).

The experimental situation regarding the spectra of high-spin states is not as good. In Fig. 8 we compare our calculations with the data on the production of resonances with spin $J \geq 2$ (Refs. 56 and 60). We see that this approach leads to a good description of the x distributions of the $f_2(1270)$ meson in Kp and pp collisions, although the accuracy of the existing data do not allow some theoretical details to be clarified.

Data on the integrated cross sections for $\rho^0(770)$-, $f_2(1270)$-, $\rho_3^0(1690)$-, and $f_4(2050)$-meson production in pp interactions at 405 GeV are given in Ref. 64. In Table I we give the theoretical and experimental cross-section ratios σ^J/σ^ρ. Our predictions agree well with the data up to spin $J = 4$.

3. HADRONIZATION OF PARTICLES WITH OPEN CHARM IN THE QUARK–GLUON STRING MODEL

3.1. Creation of particles with open charm taking into account the contributions from decays of resonance states

In this section we shall discuss a modification of the quark–gluon string model for calculating charmed-particle spectra including decays of S-wave resonances such as 1^- mesons (D^* and D_s^*) and $\frac{1}{2}^+$ (Σ_c and Ξ_c') and $\frac{3}{2}^+$ (Σ_c^*, Ξ_c^*, and Ω_c^*) hyperons.[35,36] The model parameters were determined from comparison with the experimental data. The contributions to the spectra of stable particles from resonance decays were taken into account according to their partial widths.[70]

In this section we shall consider only the spectra integrated over the transverse momentum $p_\perp$ of the created particle. We shall include the decay of S-wave charmed resonances into stable charmed particles with the emission also of π mesons or γ quanta.[70] The kinematics of these decays are described as in Ref. 71. With our assumptions, the invariant cross section for producing the hadron h has the form

$$x\frac{d\sigma^h}{dx} = x\frac{d\sigma^{h\,\mathrm{dir}}}{dx} + \sum_R \int_{x_-^*}^{x_+^*} x_R \frac{d\sigma^R}{dx_R}\Phi(x_R)dx_R. \qquad (70)$$

Here $x d\sigma^{h\,\mathrm{dir}}/dx$ is the cross section for direct production of the hadron h, and $x_R d\sigma^R/dx_R$ is the cross section for producing the resonance R. The function $\Phi(x_R)$ describes the two-particle decay of the resonance R into the hadron h. After integrating over the transverse momentum of both the hadron h and the resonance R, the function $\Phi(x_R)$ has the form

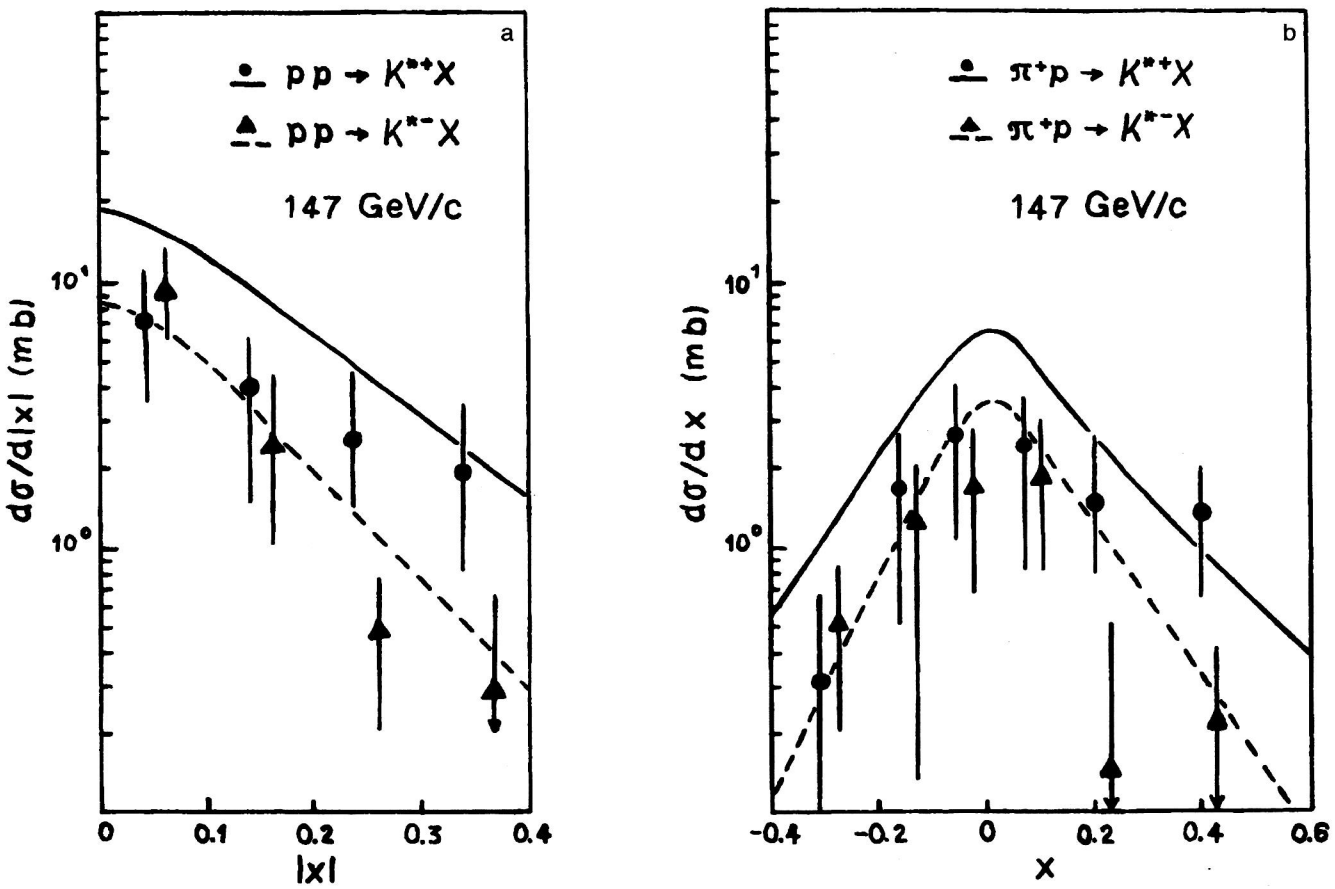

FIG. 7. Predictions of the quark–gluon string model and data[57] on the production of charged $K^{*\pm}$ mesons in $\pi^+ p$ and pp collisions.

$$\Phi(x_R)=\frac{M_R}{2p^*}\frac{1}{x_R^2}. \tag{71}$$

In (70) and (71), x_R is the Feynman variable of the resonance R,

$$x_+^*=\frac{M_R\tilde{x}}{E^*-p^*}, \quad x_-^*=\frac{M_R\tilde{x}}{E^*+p^*},$$

$$\tilde{x}=\sqrt{x^2+x_\perp^2}, \quad x_\perp=\frac{2\sqrt{\langle p_\perp^2\rangle+m^2}}{\sqrt{s}}, \tag{72}$$

m is the mass of the created hadron h, M_R is the resonance mass, E^* and p^* are the energy and 3-momentum of the hadron h in the resonance rest frame, and $\langle p_\perp^2\rangle$ is the average transverse momentum of the hadron h. The expressions for the invariant cross section for producing the hadron h are given in Sec. 2 above. Here we shall give only the expressions for the functions $f_q^h(x,n)$ for a Σ^- beam, expressed in terms of the corresponding functions of the s- and d quarks, $f_s^h(x,n)$ and $f_d^h(x,n)$:

$$f_q^{h(\Sigma^-)}(x,n)=\frac{1}{3}f_s^{h(\Sigma^-)}(x,n)+\frac{2}{3}f_d^{h(\Sigma^-)}(x,n),$$

$$f_q^{h(\Xi^-)}(x,n)=\frac{2}{3}f_s^{h(\Xi^-)}(x,n)+\frac{1}{3}f_d^{h(\Xi^{-1})}(x,n). \tag{73}$$

In the additive quark model, a diquark in an S-wave baryon can have spin (isospin) 0 and 1. Therefore, the diquark function $f_{qq}^h(x)$ can be expressed in terms of the scalar (0) and vector (1) diquark functions with weights determined by the $SU(6)$-symmetric functions:[72]

$$f_{qq}^{h(p)}=\frac{1}{3}f_{uu}^{h(p)}(x,n)+\frac{1}{2}f_{(ud)_0}^{h(p)}(x,n)+\frac{1}{6}f_{(ud)_1}^{h(p)}(x,n),$$

$$f_{qq}^{h(\Sigma^-)}=\frac{1}{3}f_{dd}^{h(\Sigma^-)}(x,n)+\frac{1}{2}f_{(ds)_0}^{h(\Sigma^-)}(x,n)+\frac{1}{6}f_{(ds)_1}^{h(\Sigma^-)}(x,n),$$

$$f_{qq}^{h(\Xi^-)}=\frac{1}{3}f_{ss}^{h(\Xi^-)}(x,n)+\frac{1}{2}f_{(ds)_0}^{(\Xi^-)}(x,n)+\frac{1}{6}f_{(ds)_1}^{h(\Xi^-)}(x,n). \tag{74}$$

We shall assume that the distribution functions of scalar and vector diquarks $u_{qq}(x,n)$ entering into the quark functions $f_i^h(x,n)$ are identical. However, different diquarks fragment into baryons in different ways. For example, direct Λ_c production in pp collisions is determined by the scalar (and isoscalar) diquark function $f_{(ud)_0}$, and direct production of the Σ_c and Σ_c^* hyperons is determined by the vector diquark function $f_{(ud)_1}$.

We shall also assume that the diquark spin does not affect diquark breakup. In the case of diquark fragmentation into mesons, this assumption leads to the equation $f_{(qq)_0}^M(x,n)=f_{(qq)_1}^M(x,n)$, and Eq. (74) reduces to

$$f_{qq}^{M(p)}(x,n)=\frac{1}{3}f_{uu}^{M(p)}(x,n)+\frac{2}{3}f_{ud}^{M(p)}(x,n),$$

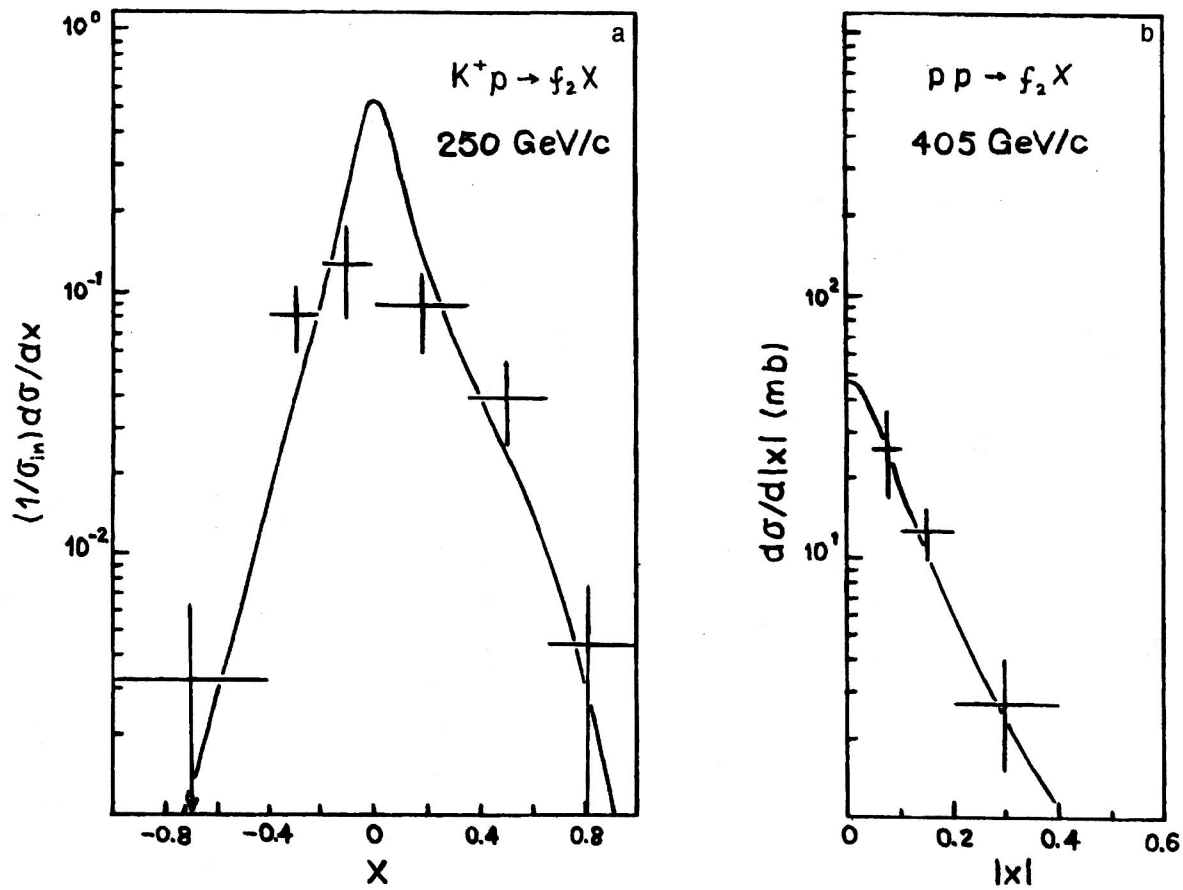

FIG. 8. Comparison of our predictions with the data on $f_2(1270)$-meson production in the processes $K^+p \to f_2X$ (Ref. 60) and $pp \to f_2X$ (Ref. 56).

$$f_{qq}^{M(\Sigma^-)}(x,n)=\frac{1}{3}f_{dd}^{M(\Sigma^-)}(x,n)+\frac{2}{3}f_{us}^{M(\Sigma^-)}(x,n),$$

$$f_{qq}^{M(\Xi^-)}(x,n)=\frac{1}{3}f_{ss}^{M(\Xi^-)}(x,n)+\frac{2}{3}f_{ds}^{M(\Xi^-)}(x,n), \qquad (75)$$

which coincides with the results of Ref. 73 for diquarks in the proton and the Σ^- hyperon.

A complete list of the quark and diquark distribution functions in π mesons, p, and the Σ^- and Ξ^- hyperons used in the present analysis is given in Appendix B. Henceforth, we shall assume that the quark and diquark fragmentation functions are independent of the spin of the captured quark (or diquark). This assumption leads to equality of the functions describing the fragmentation of the corresponding quark or diquark into the Σ_c, Σ_c^*, Ξ_c', and Ξ_c^* baryons and the D and D^* mesons. The method of parametrizing the fragmentation functions used in this section differs slightly from that used earlier (see Refs. 25, 26, 29, and 33). We shall represent the fragmentation function as the sum of two terms. The first is the product of two polynomials, each corresponding to the sum of all possible asymptotic and preasymptotic terms in the fragmentation [$x \to 1$, expansion in powers of $(1-x)$] and central ($x \to 0$, expansion in powers of x) regions. The second represents the case where neither the fragmenting object nor any of its constituents enters into the created baryon. In the case of nonleading fragmentation, the corresponding functions contain only the second term. A complete list of functions describing quark and diquark fragmentation into Λ_c, Σ_c, Σ_c^-, Ξ_c, Ξ_c', Ξ_c^*, Ω_c, and Ω_c^* baryons and D, D^*, D_s, and D_s^* mesons is given in Ref. 35.

TABLE I. Ratios of the cross sections for processes $pp \to JX$.

σ^J/σ^ρ	Theory	Experiment
f_2/ρ^0	0.38	0.38±0.19
ρ_3^0/ρ^0	0.21	0.19±0.12
f_4/ρ^0	0.13	0.17±0.12

The quark–gluon string model with the proposed modification has been used to describe a large amount of experimental data on the inclusive spectra of the hadroproduction of charmed mesons and baryons.[74–90]

The spectra of Λ_c baryons in π^-p collisions at 230 GeV/c (Ref. 74) and pp collisions at $\sqrt{s}=63$ GeV/c (Refs. 75 and 76) are given in Figs. 9a and 9b, respectively. The dotted line in Fig. 9b shows the contribution of direct Λ_c production. We see that the agreement with the data on π^-p scattering is better. Regarding the data[75,76] on pp collisions, we see a significant difference between those of the two groups.[75,76] This makes it impossible to uniquely fix the model parameters. In Figs. 10a–10d the experimental data on the x_F dependence of leading (D^- and D^0) and nonleading (D^+ and $\bar{D}^0$) charmed mesons in π^-p interactions at

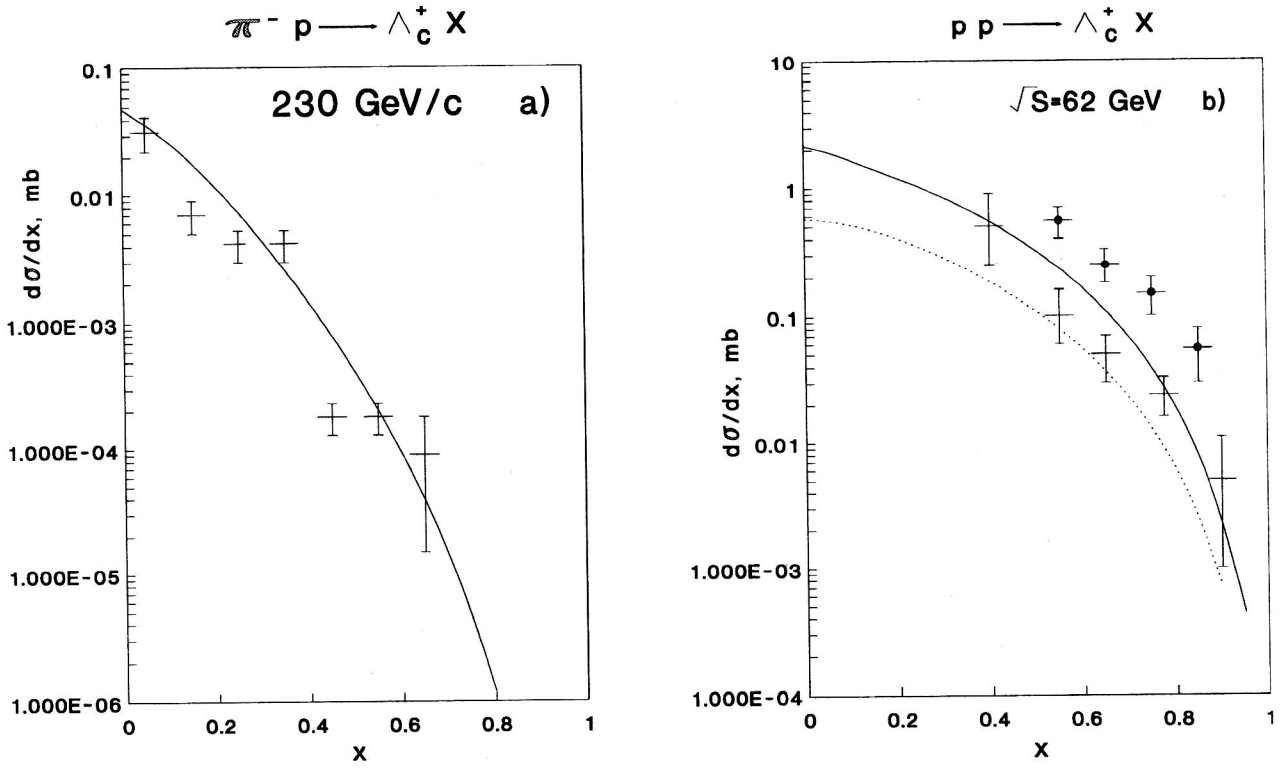

FIG. 9. Comparison of the calculations using the quark–gluon string model with the experimental data on the Λ_c spectra in (a) $\pi^- p \to \Lambda_c X$ at $p_i = 230$ GeV/c (Ref. 87) and (b) $pp \to \Lambda_c X$ at $\sqrt{s} = 63$ GeV/c (Refs. 74 and 75).

200 GeV/c (Ref. 77) and 360 GeV/c (Ref. 78) are compared with the theoretical results.

In Table II we present the data on the total cross sections for production of the Λ_c^+ baryon in pp and πp collisions and also the model calculations, in Table III we present the cross sections for D mesons, and in Table IV we give those for D^* mesons.

The predictions for the inclusive spectra of Λ_c^+, Σ_c^0, Ξ_c^+, and $D^{+/-}$ in $\Sigma^- p$ collisions are compared with the preliminary WA89 data[86] at 330 GeV/c in Figs. 11a–11d. The experimental data on Λ_c^+ and Σ_c^0 (Figs. 11a and 11b) were normalized by using the data on the total cross sections given in Ref. 86. The $D^{+/-}$ data (Fig. 11d) were normalized by using the differential distributions[87] and the data on the total D^- cross section and the cross-section ratio D^+/D^- (Ref. 86). Since the total cross sections are not available, for the Ξ_c^+ spectra (Fig. 11c) the experimental data[86] were normalized to the theoretical curve. The data on the total cross sections and the cross-section ratios for a hyperon beam are compared in Tables V and VI. In Table V we also give the predictions for the total cross sections for Ξ_c^+ and Ξ_c^0 production.

3.2. The problem of internal charm in the quark–gluon string model

The results presented in the preceding section were calculated neglecting the contribution of internal charm in the π meson or proton. Calculations of the spectra and the total cross sections in the quark–gluon string model (see, for example, the literature cited in Ref. 25) show that the present accuracy of the experimental data on the production of hadrons with hidden charm does not require the use of this hypothesis. The internal-charm hypothesis was proposed by Brodsky[91] to describe the spectra in heavy-hadron production at large $x \to 1$. In the quark–gluon string model, c quarks can be included only as sea quarks. This was first done in Ref. 26 in describing the spectra of D mesons and Λ_c baryons. However, the recent data on the asymmetry of the production of leading and nonleading hadrons in $\pi^- p$ collisions,[88–90]

$$A(x) = \frac{d\sigma^{D^-}/dx - d\sigma^{D^+}/dx}{d\sigma^{D^-}/dx + d\sigma^{D^+}/dx}, \tag{76}$$

became more critical for determining the quantitative contribution of internal charm in the quark–gluon string model. It has been shown[92] that analysis of the asymmetry data requires changing the parameter values obtained earlier from comparison with only the data on the cross sections,[33,34] and it was concluded that the contribution of the c-quark sea is small in the quark–gluon string model. In Ref. 93 the behavior of the asymmetry $A(x)$ was described by the modification of the quark–gluon string model studied in the present section with the fragmentation functions given in Appendix C. The results of the calculations are compared with the WA82,[88] E769,[89] and E791 data[90] in Fig. 12. The solid line in that figure shows the result of the calculation without the contribution of the charmed sea, and the dashed line shows the contribution with the c-quark sea. The charmed sea was included like the contribution of the strange sea in (51) of

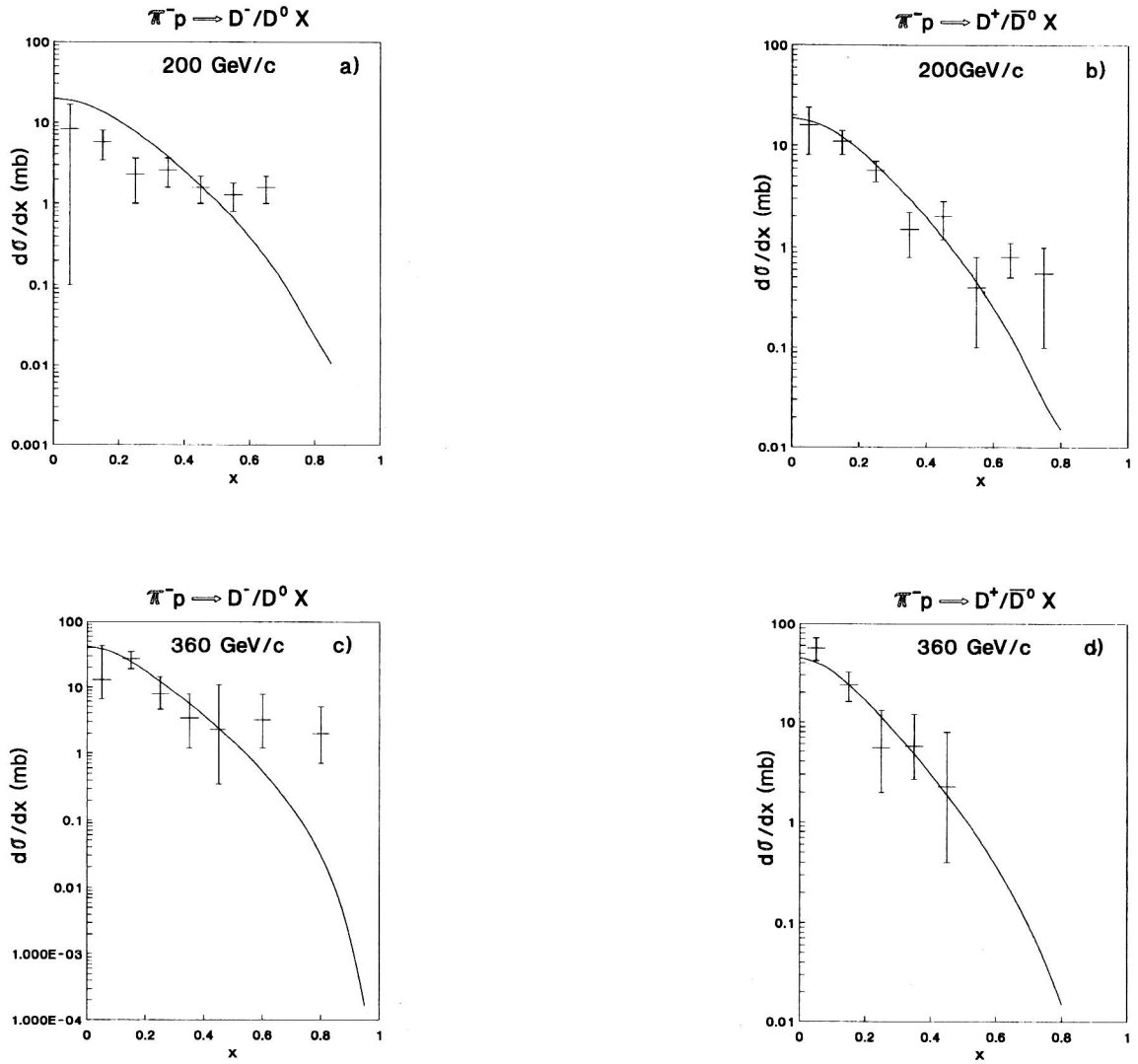

FIG. 10. Comparison of the model calculations and the experimental data on the production of leading (D^-/D^0) and nonleading ($D^+/\bar{D}^0$) charmed mesons in $\pi^- p$ interactions: (a) leading, 200 GeV/c (Ref. 82); (b) nonleading, 200 GeV/c (Ref. 82); (c) leading, 360 GeV/c (Ref. 77); (d) nonleading, 360 GeV/c (Ref. 77).

Sec. 2, with the parameter values $a^D=0.0072$, $a_1=2$, and $\delta_c=0.005$. We also studied the possibility of a different parametrization of the function $G_d^{D^-}$:

$$G_d^{D^-}(z)=(1-z)^{-\alpha_\psi(0)+\lambda}(1+a_1^D z^4). \tag{77}$$

TABLE II. Comparison of the experimental cross sections on Λ_c production in pp and πp interactions with the results of our calculations.

Reaction	Reference	P_L (GeV/c) or $\sqrt{s}$ (GeV)	$\sigma_{exp}(\mu b)$	$\sigma_{theor}(\mu b)$
$pp\to\Lambda_c X$ all x	75	63 GeV	40±18 204±11 2046±836	660
$pp\to\Lambda_C X$ $\lvert x\rvert>0.5$	76	63 GeV	101±18±26	84
$\pi^- N\to\Lambda_c X$ $x_c>0$	74	230 GeV/c	4.9±1.4±0.7	6.8

TABLE III. Comparison of the experimental cross sections on D-meson production in pp and πp interactions with the results of our calculations.

Reaction	Reference	P_L (GeV/c)	σ_{exp} (μb)	σ_{theor} (μb)
$pp\to D^+X$	82	400	5.7±1.5	4.16
$pp\to D^-X$	82	400	6.2±1.1	5.54
$pp\to D^0X$	82	400	10.5±1.9	7
$pp\to\bar{D}^0X$	82	400	7.9±1.5	12.3
$pp\to D^+/D^-X$	83	800	33±7	22.2
$pp\to D^0/\bar{D}^0X$	83	800	26^{+21}_{-13}	45.4
$pp\to D^+/D^-X$	84	800	26±14	22.2
$pp\to D^0/\bar{D}^0X$	84	800	22^{+4}_{-7}	45.4
$pN\to D/\bar{D}X$ $x_F>0$	77	200	1.5±0.7±0.1	5.6
$\pi^- N\to D^+/D^-X$	77	200	$1.7^{+0.4}_{-03}\pm0.1$	3.5
$\pi^- N\to D^0/\bar{D}^0X$	77	200	$3.3^{+0.5}_{-0.4}\pm0.3$	5.3
$\pi^- N\to D^-/D^0X$	77	200	$2.3^{+0.4}_{-03}\pm0.1$	4.7
$\pi^- N\to D^+/\bar{D}^0X$	77	200	$3.2^{+0.5}_{-0.4}\pm0.2$	4.2
$\pi^- p\to D^+/D^-X$	79, 78	360	5.7±1.5	7.76
$\pi^- p\to D^0/\bar{D}^0X$	79, 78	360	10.1±2.2	11.0

TABLE IV. Experimental data and model calculations for D^* and D_s production in πp and pp collisions.

Reaction	Reference	P_L (GeV/c)	σ_{exp} (μb)	σ_{theor} (μb)
$pp\to D^{*+}/D^{*-}X$	82	400	9.2 ± 2.4	7.14
$pp\to D^{*0}/\bar{D}^{*0}X$	82	400	5.8 ± 2.7	8.8
$\pi^-p\to D^{*+}/D^{*-}X$	80	360	$5.0^{+2.3}_{-1.8}$	5.0
$\pi^-p\to D^{*0}/\bar{D}^{*0}X$	80	360	7.3 ± 2.9	4.5
$\pi^-N\to D^{*+}/D^{*-}X$	77	200	$2.4\pm0.4\pm0.2$	2.6
$pp\to D_s^+/D_s^-X$ $x_F>0$	82	400	<2.5	2.8

TABLE V. Experimental data[86,87] on the total cross sections in Σ^-p collisions and the results of our calculations.

Particle	Region of x_F	$\sigma_{exp}(\mu b)$	$\sigma_{theor}(\mu b)$
D^-	>0.1	$2.9\pm0.8\pm0.6$	2.18
Λ_c^+	>0.2	$9.3\pm4.3\pm2.5$	10.0
Σ_c^0	>0.2	$4.8\pm2.6\pm1.5$	5.2
Ξ_c^0	>0.2		6.0
Ξ_c^+	>0.2		0.9

The result of calculating the behavior of the asymmetry using the function (77) is shown by the dot-dash line in Fig. 12. We see that finding the contribution of the charmed sea is strongly related to the parametrization of the fragmentation function, and it cannot be uniquely determined from the existing data on D-meson production.

4. SEMIHARD HADRONIC PROCESSES AND THE QUARK–GLUON STRING MODEL

4.1. The basic formalism

As shown, in particular, above, soft hadronic processes can be described very well by the Regge model combined with QCD ideas.

In recent years a great deal of work has been done to attempt to broaden the region where this nonperturbative approach is applicable for describing semihard and hard hadronic processes. One example is the two-component dual topological unitarization model.[102–104] The two components are the soft one, based on the theory of the supercritical Pomeron (the soft Pomeron), and the hard one described by perturbative QCD (the hard Pomeron); the model also includes diffraction processes. In this model (as in the quark–gluon string model) the cut Pomeron is represented as two quark–gluon chains (or strings) connecting the hadron constituents. In a first approximation the proton consists of a single valence quark and a single valence diquark, and the interaction between the hadrons leads to the existence of two strings connecting these constituents. The secondary-particle

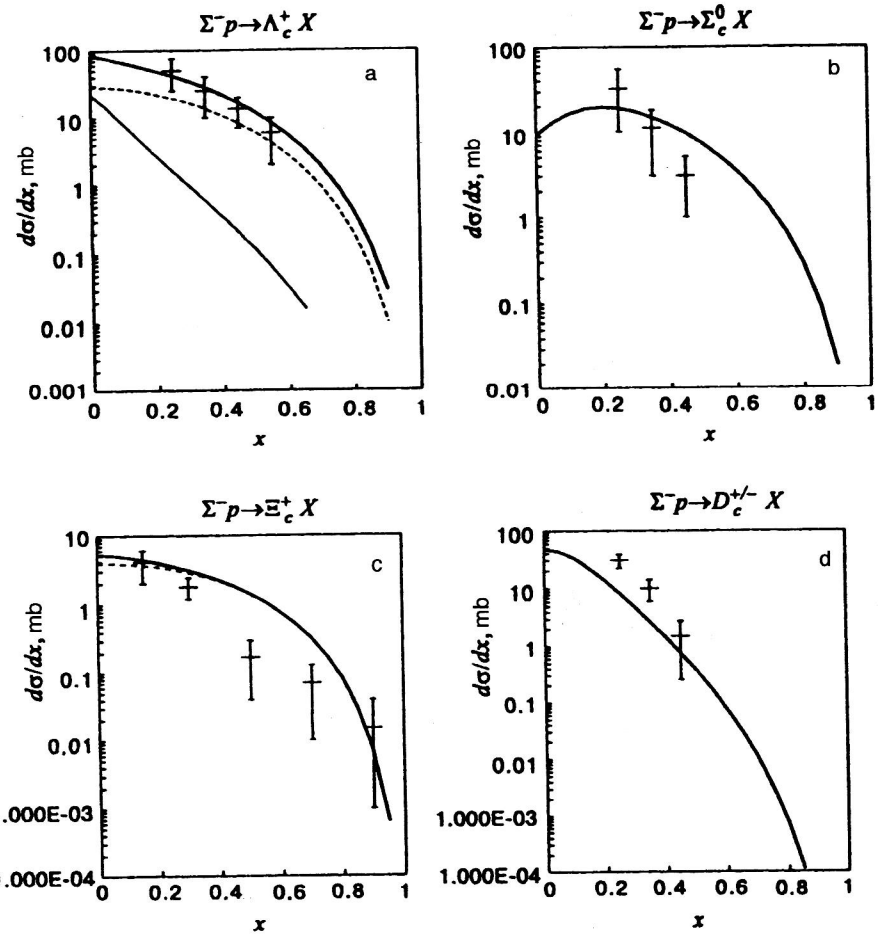

FIG. 11. Comparison of the model calculations with the preliminary experimental data[86] on the inclusive spectra of (a) Λ_c (heavy line—all Λ_c, thin line—direct Λ_c, dashed line—Λ_c from Σ_c^0 decay; (b) Σ_c^+; (c) Ξ_c^+ (heavy line—all, thin line—from Ξ_c^{*0}); (d) $D^+ + D^-$ in Σ^-p collisions at 330 GeV/c.

TABLE VI. Comparison of the experimental data[86] on the cross-section ratios in $\Sigma^- p$ collisions with the results of our calculations.

Ratio	Region of x_F	Exp. value	Model pred.
Λ_c/D^-	>0.2	11.34±7.1	12.5
Σ_c^{++}/Σ_c^0	>0.2	<0.52	0.001
Σ_c^0/Λ_c	>0.2	0.45±0.31	0.52
D^+/D^-	>0.1	0.47±0.14	0.55

multiplicities are calculated in the unitarization scheme using the Abramovskiĭ–Gribov–Kancheli sum rules.[105] Regarding the hard Pomeron, in this model it is represented by two perturbative gluons in hard quark scattering 2→2. The hard scattering mechanism is included when the gluon transverse momenta are greater than 2 or 3 GeV/c; then these gluons break up into $q\bar{q}$ pairs. The partons at the ends of the hard or semihard chain have the transverse momenta predicted by perturbative QCD.

Particle multiple production is nonperturbative in nature and, unfortunately, at present cannot be studied by using perturbative QCD. High-energy hadron–hadron interactions are dominated by Pomeron exchange, and the concept of Pomeron exchange is used in Regge models of multiple production. It is expected that these models can be explained by perturbative QCD. Several attempts are being made at present to derive the Pomeron by using perturbative QCD.[106–108] Here the main problem is not so much the value of the coupling constant as the infrared singularities which arise in the quark and gluon propagators.

The exchange of a phenomenological Pomeron can be

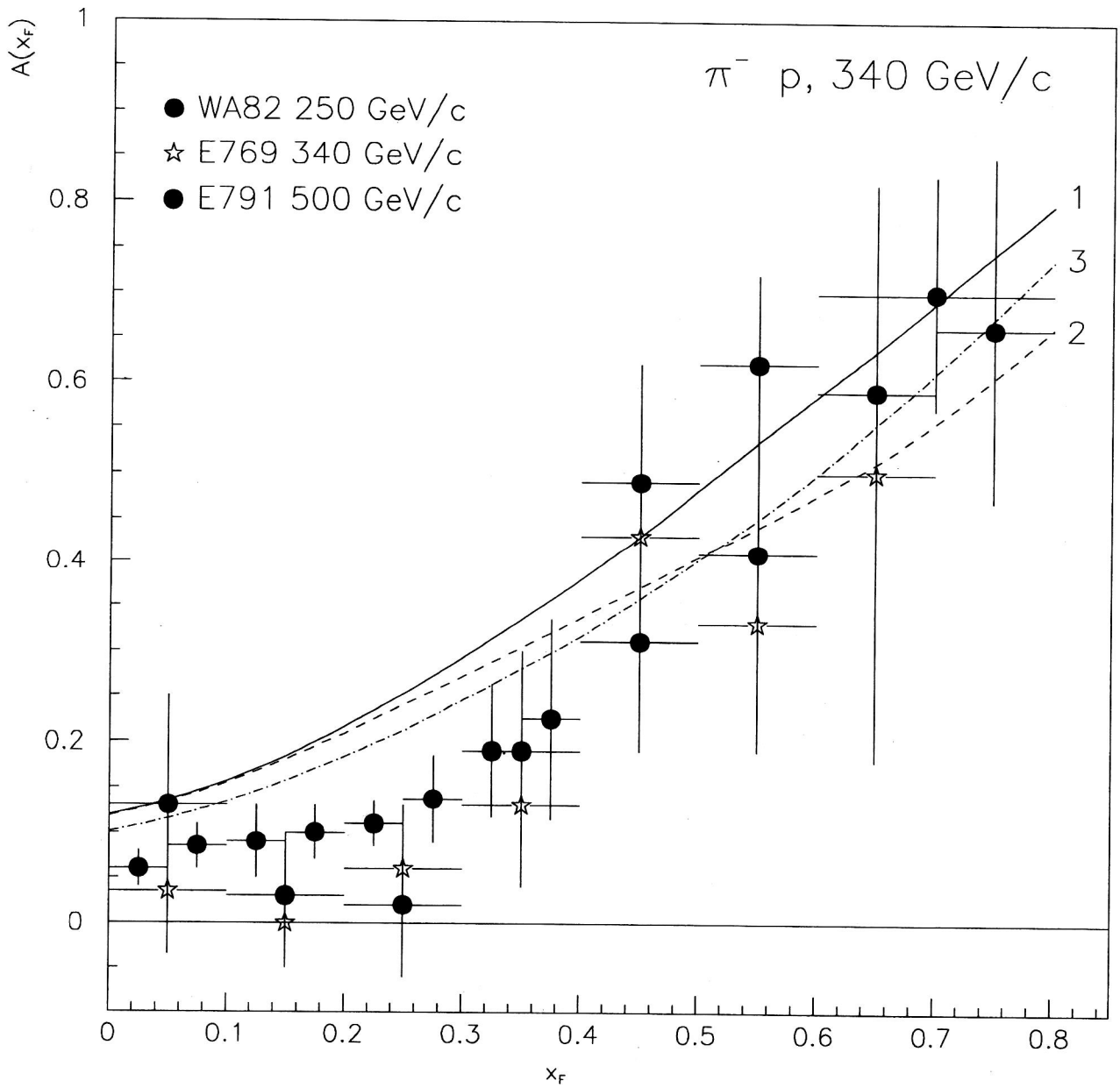

FIG. 12. Comparison of the theoretical calculations with the experimental data[88,89] on the dependence of the asymmetry of producing leading (D^-) and nonleading (D^+) mesons on x_F in $\pi^- p$ interactions.

understood as the exchange of two gluons.[106,108] However, calculations of the amplitude of quark elastic scattering using perturbative QCD lead to a singularity at zero 4-momentum transfer $t=0$. This singularity originates in the pole of the gluon propagator at $q^2=0$, and so it is clear that the behavior of the cross section at small t cannot be explained within perturbative QCD. However, the singularity in two-gluon calculations of hadron–hadron scattering is eliminated if the gluon propagator is bounded at $q^2=0$ (Ref. 107).

Behavior of the gluon propagator at small q^2 less singular than a pole occurs when studying QCD vacuum effects leading to confinement.[107] For example, in the Landshoff–Nachtmann model,[107] the Pomeron is constructed as the exchange of two nonperturbative gluons, where a nonperturbative gluon is one whose propagator does not have a pole at $q^2=0$. In a different study,[109] an approximate solution of the Schwinger–Dyson equation in the axial gauge was obtained for the gluon propagator. The behavior of this solution at $q^2=0$ turned out to be less singular than a pole at this point. The use of this propagator[109] in the Landshoff–Nachtmann model leads, as shown in Ref. 107, to good agreement between the calculations and the data.

Another approximate solution of the Schwinger–Dyson equation was obtained in Ref. 110. In this solution the gluon propagator is regularized by a dynamically generated gluon mass. In contrast to the solution of the Schwinger–Dyson equation obtained earlier,[109] the propagator with dynamical gluon mass asymptotically satisfies the renormalization-group equation and is actually bounded for $q^2=0$ (owing to the presence of an effective gluon mass). The use of this propagator in the Landshoff–Nachtmann model shows that the Pomeron effectively behaves like photon exchange, with the coupling constant determined by the gluon mass. This approach allowed the total and elastic differential cross sections $(d\sigma/dt)$ for pp scattering to be calculated, and good agreement was obtained between the calculations and the data for gluon mass $m_g=370\,\text{MeV}$ and $\Lambda_{\text{QCD}}=300\,\text{MeV}$ (Ref. 111).

In this section we shall study the possibility of modifying the quark–gluon string model so as to describe semihard hadronic processes.[44,45] For this the Pomeron is represented as the exchange of two gluons with dynamically generated mass.[107] The propagator of the corresponding nonperturbative gluon is iteratively used in n-Pomeron chains to calculate the transverse-momentum distribution of the quarks at the ends of quark–gluon strings. This process of successively including more and more Pomeron exchanges leads to an increase of the resulting transverse momentum of the secondary hadron. The dependence on the particle transverse momenta introduced in this manner does not change the standard quark–gluon string model describing the particle longitudinal-momentum distribution, while it extends the region of applicability of the model to transverse momenta of 4–5 GeV/c. The modified quark–gluon string model is used to describe the invariant cross sections and transverse-momentum distributions of secondary mesons at various initial energies.

4.2. The Pomeron as two-gluon exchange and the quark transverse momenta

In the Landshoff–Nachtmann model,[107] Pomeron exchange between two quarks behaves like a graph with single-photon exchange. The Pomeron–quark coupling constant is given by

$$\beta_0^2=\frac{1}{36\pi^2}\int d^2q[g^2D(q^2)]^2, \tag{78}$$

where $D(q^2)$ is the gluon propagator. The advantage of using a propagator bounded at $q^2=0$ is that the integral (78) converges. This does not occur for most of the solutions of the Schwinger–Dyson equation obtained by other authors.[109,112] The phenomenological value $\beta_0=2\,\text{GeV}^{-1}$ is determined from the total cross section and corresponds to the gluon mass $m_g=1.2\Lambda_{\text{QCD}}$, $\Lambda_{\text{QCD}}=300\,\text{MeV}$ (Ref. 111). It proved possible to describe the experimental data on forward proton–proton scattering for these parameter values.[111]

A gluon with bare mass leads to violation of unitarity and gauge invariance. This problem can be avoided in the case of a dynamically generated gluon mass.[111] The fact that the gluon behaves as a massive particle is also indicated by lattice calculations.[113] The approximate solution of the Schwinger–Dyson equation in a partial gauge does not lead to generation of a dynamical gluon mass.[109,112] Meanwhile, a gauge-invariant set of graphs for the Schwinger–Dyson equation has been found[110] which gives an expression for the gluon propagator which is bounded for $q^2=0$. This solution has the correct asymptotic behavior of the propagator at large q^2 and satisfies the renormalization-group equation.

In the Feynman gauge the gluon propagator with dynamical mass is given by $D_{\mu\nu}=-ig_{\mu\nu}D(q^2)$ (Ref. 110), where

$$D^{-1}(q^2)=b_0g^2[q^2+m^2(q^2)]\ln(S^2/\Lambda^2),$$

$$S^2=q^2+4m^2(q^2),$$

$$m^2(q^2)=m_g^2\left[\frac{\ln((q^2+4m_g^2)/\Lambda^2)}{\ln(4m^2/\Lambda^2)}\right]^{-12/11} \tag{79}$$

Here m_g is the gluon mass, $b_0=(33-2n_f)/48\pi^2$ is the leading coefficient of the β function in the renormalization-group equation, and the coupling constant g is fixed. The solution (79) is real when $m_g>\Lambda/2$.

We shall represent secondary-hadron production as follows. The incident proton and target nucleon break up into a quark and diquark with oppositely directed transverse momenta. At the instant of the color interaction between the quark of the incident proton and the diquark of the target nucleon, exchange of a soft massive gluon occurs. The analogous exchange of a second massive gluon occurs independently of this in the second chain. Then, after this gluon exchange the two strings formed decay into secondary hadrons. This process is repeated n times in the production of n Pomeron showers (or $2n$ quark–antiquark chains). As a result, the quark (diquark) at the ends of each string acquires nonzero transverse momentum, which is larger, the more gluon exchanges there are. The procedure for calculating the

quark (diquark) distribution after the first two-gluon exchange can be represented mathematically as follows.

We write the quark (diquark) distribution in the initial protons in factorized form:

$$\tilde{f}_\tau(x,\vec{k}_\perp)=f_\tau(x)g_0(\vec{k}_\perp), \tag{80}$$

where the quark transverse-momentum distribution is chosen to be a Gaussian normalized to unity,

$$g_0(\vec{k}_\perp)=\frac{\gamma}{\pi}\exp(-\gamma\vec{k}_\perp^2). \tag{81}$$

After the exchange of a gluon with dynamical mass, the quark distribution in the first chain will have the form

$$g_1(\vec{k}_{1\perp})=\int g_0(\vec{k}_\perp)D^2[(\vec{k}_{1\perp}-\vec{k}_\perp)^2]d^2k_\perp. \tag{82}$$

The quark distribution in the second chain will have a similar form.

After the exchange of the second gluon, the quark distribution will be expressed in terms of the function $g_1(\vec{k}_{1\perp})$:

$$g_2(\vec{k}_{2\perp})=\int g_1(\vec{k}_{1\perp})D^2[(\vec{k}_{2\perp}-\vec{k}_{1\perp})^2]d^2k_{1\perp}. \tag{83}$$

Repeating this iteration procedure, we obtain the quark distribution function in the nth chain, expressed in terms of the function $g_{n-1}(\vec{k}_{n-1\perp})$ and, in the end, in terms of the function $g_0(\vec{k}_\perp)$:

$$\begin{aligned}g_n(\vec{k}_{n\perp})&=\int g_{n-1}(\vec{k}_{n-1\perp})D^2[(\vec{k}_{n\perp}-\vec{k}_{n-1\perp})^2]d^2k_{n-1\perp}\\&=\int d^2k_{n-1\perp}D^2[(\vec{k}_{n\perp}-\vec{k}_{n-1\perp})^2]\\&\times\int d^2k_{n-2\perp}D^2[(\vec{k}_{n-1\perp}-\vec{k}_{n-2\perp})^2]\ldots\\&\cdot\int d^2k_{0\perp}D^2[(\vec{k}_{1\perp}-\vec{k}_{0\perp})^2]g_0(\vec{k}_{0\perp}).\end{aligned} \tag{84}$$

Obviously, in an n-Pomeron chain the quark functions will also be factorized:

$$\tilde{f}_\tau^{(n)}(x_n,\vec{k}_{n\perp})=f_\tau^{(n)}(x_n)g_{\tau\to h}^{(n)}(\vec{k}_{n\perp}), \tag{85}$$

Let us now turn to the construction of the invariant inclusive spectrum of the created hadrons, taking into account its dependence both on x and on the transverse momentum p_t. The expression for the hadron invariant inclusive spectrum can be written as[38–41]

$$E\frac{d\sigma}{d^3\vec{p}}=\sum_{n=0}^{\infty}\sigma_n(s)\varphi_n(x,p_\perp), \tag{86}$$

where $\varphi_n(x,p_\perp)$ is the distribution in the Feynman variable x and the transverse momentum $p_\perp$ of hadrons produced in the decay of an n-Pomeron chain.

The functions $\varphi_n(x,p_\perp)$ are represented as[39,41]

$$\varphi_n(x,p_\perp)=\int_{x_+}^1 dx_1\int_{x_-}^1 dx_2\Psi_n(x,p_\perp;x_1,x_2), \tag{87}$$

where

$$\begin{aligned}\Psi_n(x,\vec{p}_\perp;x_1,x_2)&=F_{qq}^{(n)}(x_+,\vec{p}_\perp;x_1)F_{q_v}^{(n)}(x_-,\vec{p}_\perp;x_2)/F_{q_v}^{(n)}(0,\vec{p}_\perp)\\&+F_{q_v}^{(n)}(x_+,\vec{p}_\perp;x_1)F_{qq}^{(n)}(x_-,\vec{p}_\perp;x_2)/F_{qq}^{(n)}(0,\vec{p}_\perp)\\&+2(n-1)F_{q_s}^{(n)}(x_+,\vec{p}_\perp;x_1)F_{\bar{q}_s}^{(n)}(x_-,\vec{p}_\perp;x_2)/\\&F_{\bar{q}_s}^{(n)}(0,\vec{p}_\perp);\end{aligned} \tag{88}$$

x_1 and x_2 are the quark (diquark) coordinates in the colliding hadrons, $x_\pm=x_\pm(n)=0.5[\sqrt{(x_n^2+x_\perp^2)}\pm x_n]$, $x_\perp=2\sqrt{(m_h^2+\vec{p}_\perp^2)}/s$; m_h is the mass of the secondary hadron, $\sqrt{s}$ is the total energy of the colliding hadrons in the c.m. frame,

$$\begin{aligned}F_\tau^{(n)}(x_\pm,\vec{p}_\perp;x_{1,2})&=\int d^2k_\perp\tilde{f}_\tau^{(n)}(x_{1,2},\vec{k}_\perp)\\&\times\tilde{G}_{\tau\to h}\left(\frac{x_\pm}{x_{1,2}},\vec{k}_\perp;\vec{p}_\perp\right),\end{aligned} \tag{89}$$

$$\begin{aligned}F_\tau^{(n)}(0,\vec{p}_\perp)&=\int_0^1 dx\int d^2k_\perp\tilde{f}_\tau^{(n)}(x,\vec{k}_\perp)\tilde{G}_{\tau\to h}(0,\vec{p}_\perp)\\&=\tilde{G}_{\tau\to h}(0,\vec{p}_\perp).\end{aligned} \tag{90}$$

The distribution $\varphi_n^h(s,y)$ depends on how the initial energy is divided among the n Pomeron showers. Let us consider two simple ways of doing this. In the first, the energy is divided equally and the role of the Feynman variable in the n-Pomeron chain is played by the quantity $x_n=nx$. The distribution $\varphi_n^h(s,y)$ in this case is[27]

$$\begin{aligned}&\varphi_n^h(s,y)=n\varphi_1^h(\xi_n,x),\\&\xi_n=\xi-2\ln(n),\quad \xi=\ln(s/s_0),\quad s_0=1\ \text{GeV}.\end{aligned} \tag{91}$$

The second version is based on successive shower emission by the leading hadron state. The function $\varphi_n^h(\xi,y)$ then has the form

$$\begin{aligned}&\Phi_n^h(s,y)=\sum_{k=1}^{n}\Phi_1^h(\xi_k,x_k),\\&\xi_k=\xi-2(k-1)\ln\frac{1}{1-x_0},\quad x_k=\frac{x}{(1-x_0)^{k-1}},\end{aligned} \tag{92}$$

where x_0 is the energy-loss parameter; at SPS energies $x_0\simeq 0.15$.

In a similar manner, the transverse momentum of the final hadron $\vec{p}_\perp$ can also be divided among n quark–gluon chains in different ways. One way was suggested in Ref. 94. There $\vec{p}_\perp$ is divided equally among these chains, as is x. In a second way proposed in Refs. 38 and 39, the hadron transverse momentum $\vec{p}_\perp$ can successively increase in going from one chain to the next. This method of dividing $\vec{p}_\perp$ among quark–gluon strings becomes especially clear in the approach considered here, where the quark and diquark or quark and antiquark interact with each other before the quark–gluon string is formed. Actually, the iteration procedure of calculating the quark (diquark) distribution $g_n(k_{n\perp})$

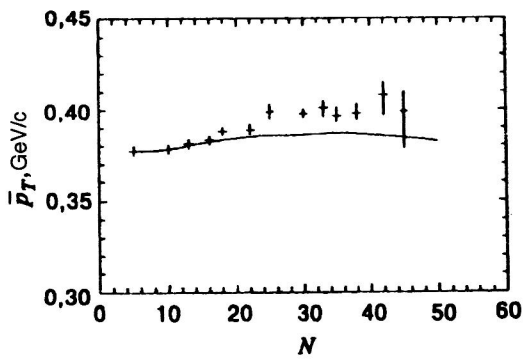

FIG. 13. Correlation of the average transverse momentum $\langle p_t \rangle$ and charged-hadron multiplicity N. The experimental data are taken from Ref. 95 at $\sqrt{s}=63$ GeV/c. The theoretical curve was calculated in the modified quark–gluon string model presented in Sec. 5.

in the transverse momentum $k_{n\perp}$ after n gluon exchanges is a reflection of the successive splitting of the transverse momentum among quark–gluon chains.

In what follows we shall mostly use this method of successively dividing x and p_t among Pomeron showers.

The fragmentation functions are written as[39–41]

$$\tilde{G}_{\tau\to h}(z_n,\vec{k}_{n\perp};\vec{p}_\perp)=G_{\tau\to h}(z_n,\vec{p}_\perp)g^n_{\tau\to h}(\tilde{k}_{n\perp}); \tag{93}$$

$$g^{(n)}_{\tau\to h}(\tilde{k}_{n\perp})=\frac{\gamma_n}{\pi}\exp(-\gamma_n\tilde{k}^2_{n\perp}), \tag{94}$$

$$\tilde{k}_{n\perp}=\vec{p}_\perp-z_n\vec{k}_{n\perp}, \quad z_n=\frac{x_\pm(n)}{x_{1,2}}. \tag{95}$$

Now substituting (84)–(95) into (89) and (90) and integrating over $d^2k_\perp$, for $F^{(n)}_\tau$ we obtain the following simple expression:

$$F^{(n)}_\tau(x_\pm(n),\vec{p}_\perp;x_{1,2})=\tilde{f}^{(n)}_\tau(x_{1,2})G_{\tau\to h}\left(\frac{x_\pm(n)}{x_{1,2}},\vec{p}_\perp\right)\times\tilde{I}_n(z_n,\vec{p}_\perp), \tag{96}$$

in which the function $\tilde{I}_n(z_n,\vec{p}_\perp)$ contains the transverse-momentum dependence:

$$\tilde{I}_{(n)}(z_n,\vec{p}_\perp)=\int d^2k_\perp\int\prod_{i=1}^{n}g_{i-1}(\vec{k}_{i-1,\perp})\times D^2[(\vec{k}_{i\perp}-\vec{q}_{i-1,\perp})^2]d^2q_{i\perp}\frac{\gamma_n}{\pi}\times\exp[-\gamma_n(\vec{p}_\perp-z_n\vec{k}_{n\perp})^2]. \tag{97}$$

4.3. Analysis of the results and comparison with the data

In Fig. 13 we show the dependence $\langle p_\perp\rangle(N)$ analyzed in the quark–gluon string model along with the introduced dependence of the quark distributions and fragmentation functions on the quark transverse momenta $k_\perp$. The details of the calculations of this observable are given in Ref. 45. The two-gluon exchange mechanism used in our model leads to a growing dependence $\langle p_\perp\rangle(N)$. However, the complete description of this characteristic requires extension of the range of applicability of the model to transverse momenta greater than 4–5 GeV/c, where the contribution of semihard effects becomes more and more important. Moreover, the expressions for the cross sections σ_n were obtained by including only the unenhanced graphs of the Reggeon theory.[52] The inclusion of enhanced graphs leads to the appearance of $1/x$ terms in the sea-quark distributions, the contribution of which is especially large for $x\simeq 0$, where the largest number of hadrons is produced. In addition, at large $p_\perp$ the contribution of new mechanisms such as hard parton scattering, not included in the present model, grows.

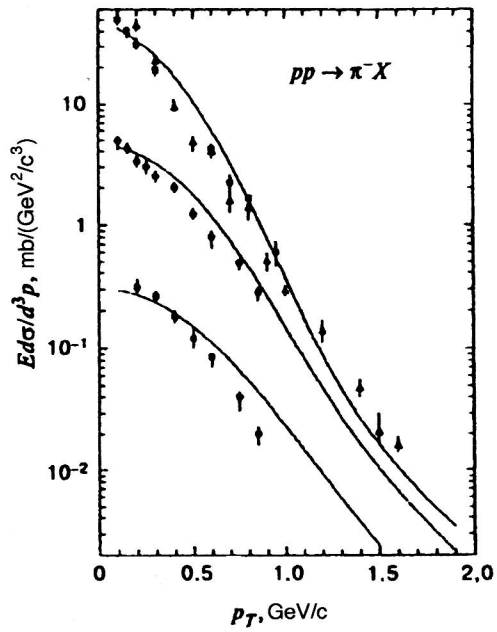

FIG. 14. Invariant inclusive spectrum of π^- mesons in pp collisions at $\sqrt{s}=19.5$ GeV/c (Ref. 114). The distributions in the transverse momentum $p_\perp$ for $x=0$, 0.3, and 0.6 are given. The curve was calculated using the modified quark–gluon string model.

Let us now consider the distributions of π mesons with large $p_\perp$ produced in high-energy pp collisions. The calculated invariant spectra $F(x,\vec{p}_\perp)$ and the corresponding experimental data[114,115] are shown in Figs. 14 and 15. We see from these figures that the version of the quark–gluon string model considered in this section gives a good description of the data for $p_\perp\leq 4.0$ GeV/c. The spectra become flatter for $p_\perp\geq 1$ GeV/c, which is characteristic of semihard processes. The rise of the cross sections at $p_\perp\geq 3$ GeV/c is perhaps related to the fact that in the model we use the values of the Regge trajectories and their derivatives at $t=0$, whereas in going to large $p_\perp$ it is necessary to include the dependence of the trajectories on the invariant variable t, $\alpha(t)$, because $t=t(p_\perp,x_F)$.

The calculated dependences of the inclusive spectra of D mesons on x_F and $p^2_\perp$ are shown in Figs. 16 and 17 together with the experimental data.[85] The data on the $p^2_\perp$ dependence of the asymmetry of producing leading (D^-) and nonleading (D^+) mesons in πp collisions[88–90] are compared with the model predictions in Fig. 18. In Ref. 39 we studied the dependence of the D-meson production cross sections on the

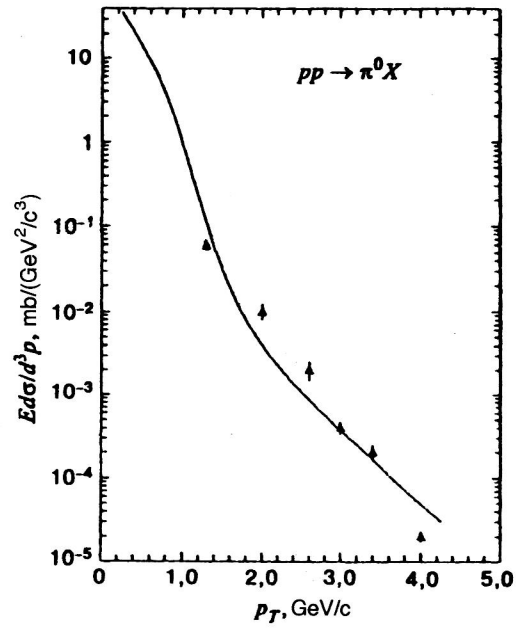

FIG. 15. Invariant inclusive spectrum of π^0 mesons in pp collisions at $\sqrt{s}=62.4$ GeV/c (Ref. 115). The curve was calculated using the modified quark–gluon string model.

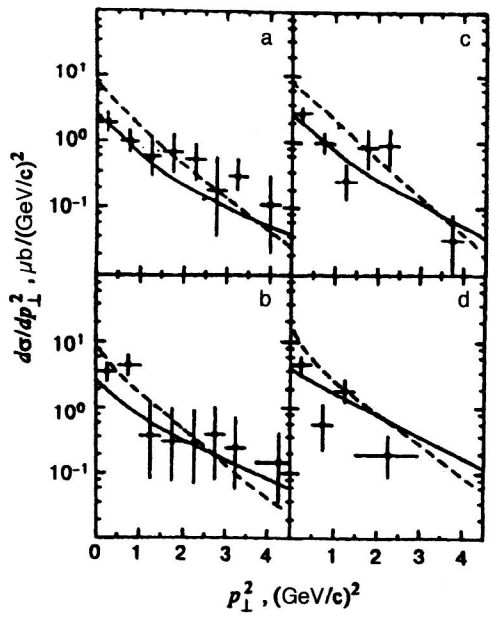

FIG. 17. $p_\perp^2$ dependence of the differential cross sections for the production of various D mesons in pp collisions.[85] The notation is the same as in Fig. 16.

intercept of the Regge trajectory of charmonium $\alpha_\psi(0)$. In the present calculations we used the intercept $\alpha(0)=0$ (Ref. 116), which implies nonlinearity of the Regge trajectories $\alpha(t)$ at $t\leq 0$ (Ref. 117). In the calculations of the present section, we took the parameters a_0 and a_1 entering into the c-quark fragmentation functions to be $a_0=10^{-4}$ and $a_1=5$ (Ref. 34).

CONCLUSION

We have studied a modification of the quark–gluon string model which includes the quark transverse motion in the colliding hadrons, and also the dependence of the fragmentation functions on the transverse momenta of the quarks and secondary hadrons. We have proposed a method of introducing the transverse-momentum dependence based on representation of the Pomeron as the exchange of two gluons with dynamically generated gluon mass. This has allowed us to determine the quark transverse-momentum distributions in quark–gluon chains and to extend the range of applicability of the quark–gluon string model to secondary-hadron transverse momenta $p_\perp \simeq 4$ GeV/c.

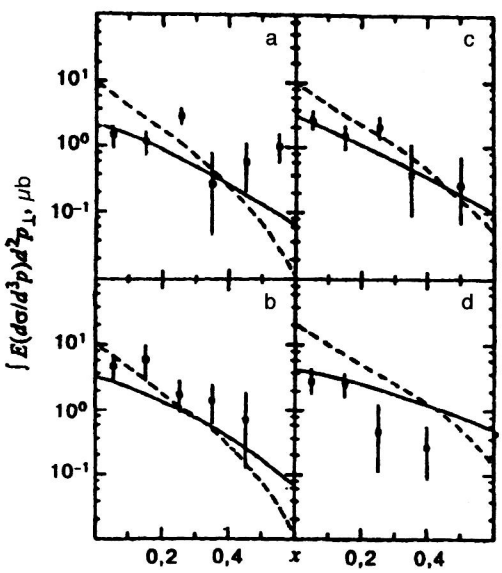

FIG. 16. x dependence of the invariant inclusive cross section for the reaction $pp \to DX$ at $\sqrt{s}=27.4$ GeV/c: (a) D^+; (b) D^0; (c) D^-; (d) $\bar{D}^0$ (Ref. 85).

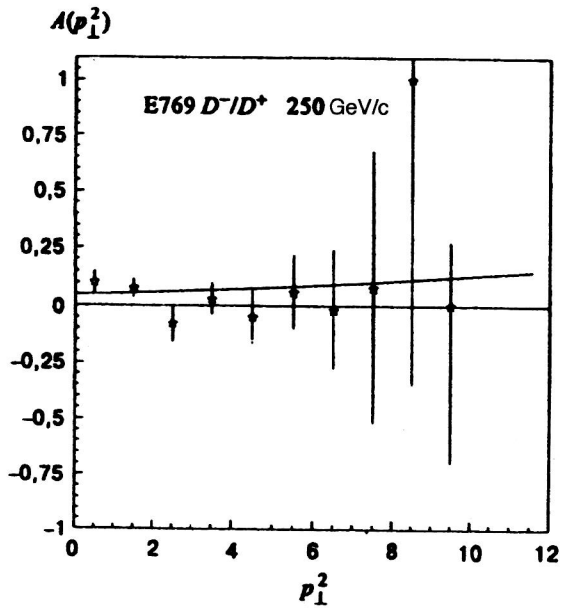

FIG. 18. Comparison of the theoretical calculations with the experimental data[88,89] on the $p_\perp^2$ dependence of the asymmetry of producing leading (D^-) and nonleading (D^+) mesons in $\pi^- p$ interactions.

We have used the model to calculate the correlations $\langle p_\perp\rangle(N)$ and the hadron invariant inclusive spectra $F(x,\vec{p}_\perp)$ for various initial energies. As we showed earlier,[40] these characteristics of hadronic processes are sensitive to how the energy and transverse momentum are divided among quark–gluon chains. The proposed method of introducing $p_\perp$ dependence into the quark–gluon string model is analogous to successive division of the energy, which appears to correspond closely to the physics of the process. Calculation of the correlation between the average hadron transverse momentum $\langle p_\perp\rangle$ and the hadron multiplicity N shows that this method of introducing the $p_\perp$ dependence effectively leads to the inclusion of semihard effects, as indicated by the growth of $\langle p_\perp\rangle(N)$ as a function of N. The manifestation of this effect in the quark–gluon string model has allowed the proposed version of the quark–gluon string model to be used to describe the D-meson distributions not only in the Feynman variable x, but also in the transverse momentum $p_\perp$. Comparison of the calculations using this version of the quark–gluon string model with the data on the D-meson yields in pp interactions provides evidence in favor of the peripheral mechanism, which is confirmed by the good agreement between the calculations and the data.

The proposed version of the quark–gluon string model gives a good description of the data at $p_\perp \leqslant 4.0$ GeV/c. The spectra are flattened for $p_\perp \geqslant 1$ GeV/c, which is characteristic of semihard processes. However, the model overestimates the differential cross sections $ds/dp_\perp^2$ at $p_\perp \geqslant 3$ GeV/c. To improve the description of the $p_\perp$ distributions in this region it is apparently necessary to use not the values of the Regge trajectories at zero, i.e., the parameters $\alpha(0)$ and $\alpha'(0)$, in the quark functions and fragmentation functions, but the Regge trajectories $\alpha(t)$ themselves and their derivatives $\alpha'(t)$, i.e., to include the dependence of the trajectories on the invariant variable t. Moreover, it is necessary to refine the quark (antiquark, diquark) transverse-momentum distributions in the colliding hadrons, since our proposed version of the quark–gluon string model uses a Gaussian distribution, which, of course, is valid only for small $p_\perp$.

We have also considered a modification of the quark–gluon string model describing the production of boson resonances. We have shown that a combination of the quark–gluon string model and the Reggeon–photon analogy can be used to obtain relations among the spectra for the production of resonances with higher spins. The proposed model gives a good description of the experimental data.

To describe the charmed-particle hadroproduction spectra, we have proposed a modification of the quark–gluon string model which also includes the contribution to the production of ground states (D mesons, Λ_c, Ξ_c, and Ω_c baryons) from decays of the corresponding S-wave resonances such as 1^- mesons (D^*) and $\frac{1}{2}^+$ (Σ_c and Ξ_c') and $\frac{3}{2}^+$ (Σ_c^*, Ξ_c^*, and Ω_c^*) hyperons.

The authors are grateful to A. V. Efremov and A. B. Kaĭdalov for useful discussions.

This study was supported by the Russian Fund for Fundamental Research. A.G.G. would also like to thank INTAS (Grant No. 93-0079) and the Armenian Fund for Fundamental Research (Grant No. 94-681) for partial support.

APPENDIX A

Let us give a complete list of the quark and diquark fragmentation functions used to describe the inclusive spectra of vector mesons. For $\rho^\pm$-meson production we have[46]

$$
\begin{aligned}
&G_u^{\rho^+}(z)=G_d^{\rho^-}(z)=b^\rho(1-z)^{-\alpha_R(0)+\lambda},\\
&G_u^{\rho^-}(z)=G_d^{\rho^+}(z)=b^\rho(1-z)^{-\alpha_R(0)+\lambda+2(1-\alpha_R(0))},\\
&G_s^{\rho^+}(z)=G_s^{\rho^-}(z)=G_{\bar{s}}^{\rho^+}(z)\\
&\qquad=G_{\bar{s}}^{\rho^-}(z)=b^\rho(1-z)^{-\alpha_R(0)+\lambda+1},\\
&G_{uu}^{\rho^+}(z)=b^\rho(1-z)^{\alpha_R(0)-2\alpha_N(0)+\lambda},\\
&G_{uu}^{\rho^-}(z)=b^\rho(1-z)^{\alpha_R(0)-2\alpha_N(0)+\lambda+1},\\
&G_{ud}^{\rho^+}(z)=G_{ud}^{\rho^-}(z)=b^\rho(1-z)^{\alpha_R(0)-2\alpha_N(0)+\lambda}\\
&\qquad\times[1+(1-z)^2]/2,
\end{aligned}
\tag{A1}
$$

where $\lambda\approx 0.5$, $\alpha_R(0)\approx 0.5$, $\alpha_N(0)\approx -0.5$, and $b^\rho\approx 0.27$ (Ref. 35).

The functions describing the fragmentation of quarks and diquarks into the ρ^0 meson have the form

$$
\begin{aligned}
&G_u^{\rho^0}(z)=G_d^{\rho^0}(z)=\frac{1}{2}[G_u^{\rho^+}(z)+G_u^{\rho^-}(z)],\\
&G_s^{\rho^0}(z)=G_{\bar{s}}^{\rho^0}(z)=G_s^{\rho^\pm}(z),\\
&G_{ud}^{\rho^0}(z)=G_{ud}^{\rho^\pm}(z),\\
&G_{uu}^{\rho^0}(z)=G_{dd}^{\rho^0}(z)=b^\rho(1-z)^{\alpha_R(0)-2\alpha_N(0)+\lambda}(1-z/2).
\end{aligned}
\tag{A2}
$$

For production of the $\omega(783)$ meson, in this approach $G_{q(qq)}^{\omega}(z)=G_{q(qq)}^{\rho^0}(z)$.

According to the results of Ref. 46, the functions $G_q^{K^*}(z)$ are written as

$$
\begin{aligned}
&G_u^{K^{*+}}(z)=G_d^{K^{*0}}(z)=b^{K^*}(1-z)^{-\alpha_\varphi(0)+\lambda}(1+b_1^K z),\\
&G_u^{K^{*-}}(z)=G_d^{\bar{K}^{*0}}(z)=G_{\bar{d}}^{K^{*+}}(z)=G_{\bar{u}}^{K^{*0}}(z)=G_{\bar{d}}^{\bar{K}^{*0}}(z)\\
&\qquad=G_{\bar{d}}^{K^{*-}}(z)=b^{K^*}(1-z)^{-\alpha_\varphi(0)+\lambda+1},\\
&G_{\bar{u}}^{K^{*-}}(z)=G_u^{K^{*+}}(z),\quad G_{\bar{u}}^{K^{*+}}(z)=G_u^{K^{*-}}(z),\\
&G_{\bar{d}}^{K^{*-}}(z)=G_d^{K^{*+}}(z),\quad G_{\bar{d}}^{K^{*+}}(z)=G_d^{K^{*-}}(z),\\
&G_{\bar{s}}^{K^{*0}}(z)=G_{\bar{s}}^{K^{*+}}(z)=G_s^{\bar{K}^{*0}}(z)\\
&\qquad=G_s^{K^{*-}}(z)=bz^{1-\alpha_\varphi(0)}(1-z)^{-\alpha_R(0)+\lambda}+b^{K^*}\\
&\qquad\times(1-z)^{-\alpha_R(0)+\lambda+2(1-\alpha_\varphi(0))},\\
&G_{\bar{s}}^{K^{*-}}(z)=G_{\bar{s}}^{\bar{K}^{*0}}(z)=G_s^{K^{*+}}(z)=G_s^{K^{*0}}(z)=b^{K^*}\\
&\qquad\times(1-z)^{-\alpha_R(0)+\lambda+2(1-\alpha_\varphi(0))}.
\end{aligned}
\tag{A3}
$$

TABLE VII.

n	π^-		p		Σ^-		Ξ^-	
i	α	β	α	β	α	β	α	β
u			$-\alpha_\rho^0$	$\alpha_\rho^0-2\alpha_N^0$	$-\alpha_\rho^0$	$\alpha_\rho^0-2\alpha_N^0+\alpha_\rho^0-\alpha_\varphi^0$	$-\alpha_\rho^0$	$\alpha_\rho^0-2\alpha_N^0+2(\alpha_\rho^0-\alpha_\varphi^0)$
d	$-\alpha_\rho^0$	$-\alpha_\rho^0$	$\alpha_\rho^0-\alpha_\rho^0+1$	$\alpha_\rho^0-2\alpha_N^0$	$-\alpha_\rho^0$	$\alpha_\rho^0-2\alpha_N^0+\alpha_\rho^0-\alpha_\varphi^0$	$-\alpha_\rho^0$	$\alpha_\rho^0-2\alpha_N^0+2(\alpha_\rho^0-\alpha_\varphi^0)$
$\bar{u}$	$-\alpha_\rho^0$	$-\alpha_\rho^0$	$-\alpha_\rho^0$	$\alpha_\rho^0-2\alpha_N^0$	$-\alpha_\rho^0$	$\alpha_\rho^0-2\alpha_N^0+\alpha_\rho^0-\alpha_\varphi^0$	$-\alpha_\rho^0$	$\alpha_\rho^0-2\alpha_N^0+2(\alpha_\rho^0-\alpha_\varphi^0)$
$\bar{d}$	$-\alpha_\rho^0$	$-\alpha_\rho^0$	$-\alpha_\rho^0$	$\alpha_\rho^0-2\alpha_N^0+1$	$-\alpha_\rho^0$	$\alpha_\rho^0-2\alpha_N^0+\alpha_\rho^0-\alpha_\varphi^0$	$-\alpha_\rho^0$	$\alpha_\rho^0-2\alpha_N^0+2(\alpha_\rho^0-\alpha_\varphi^0)$
s	$-\alpha_\varphi^0$	$-\alpha_\varphi^0$	$-\alpha_\varphi^0$	$\alpha_\rho^0-2\alpha_N^0+\alpha_\rho^0-\alpha_\varphi^0$	$-\alpha_\varphi^0$	$\alpha_\rho^0-2\alpha_N^0$	$-\alpha_\varphi^0$	$\alpha_\rho^0-2\alpha_N^0+\alpha_\rho^0-\alpha_\varphi^0$
$\bar{s}$	$-\alpha_\varphi^0$	$-\alpha_\varphi^0$	$-\alpha_\varphi^0$	$\alpha_\rho^0-2\alpha_N^0+\alpha_\rho^0-\alpha_\varphi^0$	$-\alpha_\varphi^0$	$\alpha_\rho^0-2\alpha_N^0+2(\alpha_\rho^0-\alpha_\varphi^0)$	$-\alpha_\rho^0$	$\alpha_\rho^0-2\alpha_N+3(\alpha_\rho^0-\alpha_\varphi^0)$
uu			$\alpha_\rho^0-2\alpha_N^0+1$	$-\alpha_\rho^0$				
dd					$\alpha_\rho^0-2\alpha_N^0$	$-\alpha_\varphi^0$		
ud			$\alpha_\rho^0-2\alpha_N^0$	$-\alpha_\rho^0$				
us					$\alpha_\rho^0-2\alpha_N^0+\alpha_\rho^0-\alpha_\varphi^0$	$-\alpha_\rho^0$	$\alpha_\rho^0-2\alpha_N^0+\alpha_\rho^0-\alpha_\varphi^0$	$-\alpha_\varphi^0$
ds								
ss							$\alpha_\rho^0-2\alpha_N^0+2(\alpha_\rho^0-\alpha_\varphi^0)$	$-\alpha_\rho^0$

For the diquark fragmentation functions we have

$$G_{uu}^{K^{*+}}(z)=b^{K^*}(1-z)^{2\alpha_R(0)-\alpha_\varphi(0)-2\alpha_N(0)+\lambda}(1+b_2^K z),$$

$$G_{ud}^{K^{*+}}(z)=b^{K^*}(1-z)^{2\alpha_R(0)-\alpha_\varphi(0)-2\alpha_N(0)+\lambda}\times[1+b_2^K z+(1-z)^2]/2,$$

$$G_{uu}^{K^{*-}}(z)=G_{uu}^{\bar{K}^{*0}}(z)=G_{uu}^{K^{*0}}(z)=b^{K^*}(1-z)^{-\alpha_\varphi(0)-2\alpha_N(0)+\lambda+2},$$

$$G_{ud}^{K^{*-}}(z)=G_{ud}^{\bar{K}^{*0}}(z)=b^{K^*}(1-z)^{-\alpha_\varphi(0)-2\alpha_N(0)+\lambda+2}\times(1-z/2),$$

$$G_{ud}^{K^{*0}}(z)=b^{K^*}(1-z)^{-\alpha_\varphi(0)-2\alpha_N(0)+\lambda+2}(1+b_2^K z/2), \tag{A4}$$

where $\alpha_\varphi(0)\approx 0$, $b^{K^*}\approx 0.15$, $b_1^K\approx 2$, $b_2^K\approx 5$, and $b\approx 0.4$.

APPENDIX B. THE QUARK AND DIQUARK DISTRIBUTION FUNCTIONS IN THE HADRONS OF THE INITIAL BEAM AND THE TARGET

The quark (diquark) distributions in the hadron h are parametrized as

$$f_i^n(x,n)=C_i x^{\alpha_i}(1-x)^{\beta_i'}, \tag{B1}$$

where $\beta_i'=\beta_i+2(n-1)(1-\alpha_\rho^0)$. The coefficient C_i in (B1) is determined from the normalization condition $\int_0^1 f_i^n(x,n)dx=1$ and is

$$C_i=\frac{\Gamma(1+\alpha)\Gamma(1+\beta')}{\Gamma(2+\alpha+\beta)}. \tag{B2}$$

Here $\Gamma(\alpha)$ is the gamma function.

The quantities α and β are expressed in terms of the intercepts of the Regge trajectories and are given in Table VII. We use the values $\alpha_\rho^0=0.5$, $\alpha_\phi^0=0$, and $\alpha_N^0=-0.5$.

The distribution of c-quark pairs in the π meson was parametrized as

$$f_{c(\bar{c})}^{(n)}=C_{c_{\text{sea}}}^{(n)}\delta_{c(\bar{c})}x_1^{-\alpha_\psi(0)}\times(1-x_1)^{\alpha_R(0)-2\alpha_N(0)+(\alpha_R(0)-\alpha_\psi(0))+n-1}, \tag{B3}$$

where x_1 is the momentum fraction of $c(\bar{c})$ quarks and $\delta_{c(\bar{c})}$ is the weight of charmed pairs in the quark sea.

APPENDIX C. FUNCTIONS DESCRIBING THE FRAGMENTATION OF QUARKS AND DIQUARKS INTO *D* MESONS

The functions describing quark and diquark fragmentation into charmed mesons have the form

$$G_u^{\overline{D^0}}=G_d^{D^-}=a_0(1-z)^{\lambda-\alpha_\psi(0)}(1+a_1z^2),$$

$$G_u^{D^-}=G_u^{D^+}=G_u^{D^0}=G_d^{D^+}=G_d^{D^0}=G_d^{\overline{D^0}}=a_0(1-z)^{\lambda-\alpha_\psi(0)+2.(1.-\alpha_R(0))}, \tag{C1}$$

$$G_{uu}^{D^+}=G_{uu}^{D^-}=G_{uu}^{D^0}=G_{ud}^{D^+}=G_{ud}^{D^0}=a_0(1-z)^{\lambda-\alpha_\psi(0)+2.(\alpha_R(0)-\alpha_N(0))+1},$$

$$G_{uu}^{\overline{D^0}}=a_0(1-z)^{\lambda-\alpha_\psi(0)+2.(\alpha_R(0)-\alpha_N(0))}\times\left(\frac{1+a_1}{2}z^2+\frac{(1-z)^2}{2}\right),$$

$$G_{ud}^{\overline{D^0}}=a_0(1-z)^{\lambda-\alpha_\psi(0)+2.(\alpha_R(0)-\alpha_N(0))}\left(\frac{1}{2}+\frac{1+a_1}{2}z^2\right). \tag{C2}$$

The parameter values are given in the corresponding sections. The function describing c-quark fragmentation into D mesons was chosen as

$$G^D_{c(\bar{c})}(z)=\frac{a^D_f}{a^D_0}\,z^3(1-z)^{-\alpha_R(0)+\lambda}. \qquad \text{(C3)}$$

where a^D_f is of order 1.

*)Supported by the Russian Fund for Fundamental Research.
**)Erevan Physics Institute, Erevan, Armenia.

[1] G. Altarelli and G. Parisi, Phys. Lett. B **126**, 298 (1977).
[2] J. Kogut and L. Susskind, Phys. Rev. D **9**, 3501 (1974).
[3] K. Wilson, Phys. Rev. D **10**, 2445 (1974).
[4] M. Creutz, *Quarks, Gluons and Lattices* [Cambridge University Press, Cambridge, 1983; Mir, Moscow, 1987].
[5] K. Werner, Phys. Rep. **232**, 87 (1993).
[6] A. B. Kaĭdalov, in *Elementary Particles* [in Russian], Vol. 2 (Moscow, 1980), p. 38; Yad. Fiz. **33**, 1369 (1981) [Sov. J. Nucl. Phys. **33**, 733 (1981)]; Phys. Lett. B **116**, 459 (1982); in *Elementary Particles* [in Russian], Vol. 2 (Moscow, 1980), p. 3.
[7] A. Capella, U. Sukhatme, C.-I. Tan, and J. Tran Thanh Van, Phys. Rep. **236**, 225 (1994).
[8] P. E. Raige and S. D. Protopopescu, Report BNL-37066, Brookhaven, New York (1986).
[9] H. U. Bengtsson and G. Ingelman, Comput. Phys. Commun. **34**, 251 (1985).
[10] B. Anderson, G. Gustafson, and B. Nilsson-Almquist, Nucl. Phys. B **28**, 289 (1987).
[11] N. S. Amelin *et al.*, Nucl. Phys. A **544**, 463c (1992); Phys. Rev. C **47**, 2229 (1993).
[12] A. V. Batunin, A. K. Likhoded, and A. N. Tolstenkov, Yad. Fiz. **42**, 424 (1985) [Sov. J. Nucl. Phys. **42**, 268 (1985)].
[13] E. M. Levin *et al.*, Yad. Fiz. **53**, 1059 (1991) [Sov. J. Nucl. Phys. **53**, 657 (1991)].
[14] K. P. Das and R. C. Hwa, Phys. Lett. B **68**, 459 (1977).
[15] T. Tashiro *et al.*, Z. Phys. C **35**, 21 (1987).
[16] R. G. Badalyan, Yad. Fiz. **47**, 220 (1988) [Sov. J. Nucl. Phys. **47**, 141 (1988)].
[17] V. V. Kiselev *et al.*, Yad. Fiz. **49**, 1100 (1989) [Sov. J. Nucl. Phys. **49**, 682 (1989)].
[18] G. 't Hooft, Nucl. Phys. B **72**, 461 (1974).
[19] G. Veneziano, Phys. Lett. B **52**, 220 (1974).
[20] M. Ciafaloni, G. Marchesini, and G. Veneziano, Nucl. Phys. B **98**, 472 (1975).
[21] G. F. Chew and C. Rosenzweig, Phys. Rep. **41**, 363 (1978).
[22] A. Casher, J. Kogut, and L. Susskind, Phys. Rev. D **10**, 732 (1974).
[23] X. Artru and G. Mennesier, Nucl. Phys. B **70**, 93 (1974).
[24] A. Casher, H. Neuberger, and S. Nussinov, Phys. Rev. D **20**, 179 (1979).
[25] Yu. M. Shabelski, Sov. Sci. Rev., Sect. A **17**, Part 2, 1 (1993); **40**, 135 (1984).
[26] Yu. M. Shabelski, Surv. High Energy Phys. **9**, 1 (1995).
[27] A. B. Kaĭdalov and K. A. Ter-Martirosyan, Yad. Fiz. **39**, 1545 (1984) [Sov. J. Nucl. Phys. **39**, 979 (1984)]; **40**, 211 (1984) [**40**, 135 (1984)].
[28] A. B. Kaidalov and O. I. Piskounova, Z. Phys. C **30**, 145 (1986).
[29] A. B. Kaĭdalov and O. I. Piskunova, Yad. Fiz. **41**, 1278 (1985) [Sov. J. Nucl. Phys. **41**, 816 (1985)].
[30] Yu. M. Shabel'skiĭ, A. B. Kaĭdalov, and K. A. Ter-Martirosyan, Yad. Fiz. **43**, 1282 (1986) [Sov. J. Nucl. Phys. **43**, 822 (1986)].
[31] Yu. M. Shabel'skiĭ, Yad. Fiz. **44**, 186 (1986) [Sov. J. Nucl. Phys. **44**, 117 (1986)]; **45**, 223 (1987) [**45**, 143 (1987)]; **49**, 1081 (1989) [**49**, 670 (1989)].
[32] G. H. Arakelyan, A. A. Grigoryan, N. Ya. Ivanov, and A. B. Kaidalov, Z. Phys. C **63**, 137 (1994).
[33] A. B. Kaĭdalov and O. I. Piskunova, Yad. Fiz. **43**, 1545 (1986) [Sov. J. Nucl. Phys. **43**, 994 (1986)].
[34] O. I. Piskunova, Yad. Fiz. **56**, No. 8, 176 (1993) [Phys. At. Nucl. **56**, 1094 (1993)].
[35] G. H. Arakelyan and P. E. Volkovytski, Z. Phys. A **353**, 87 (1995).
[36] G. H. Arakelyan and P. E. Volkovytski, Yad. Fiz. **59**, 1710 (1996) [Phys. At. Nucl. **59**, 1655 (1996)].
[37] K. G. Boreskov and A. B. Kaĭdalov, Yad. Fiz. **37**, 174 (1983) [Sov. J. Nucl. Phys. **37**, 100 (1983)].
[38] G. I. Lykasov and N. V. Slavin, Yad. Fiz. **49**, 1446 (1989) [Sov. J. Nucl. Phys. **49**, 898 (1989)].
[39] G. I. Lykasov and M. N. Sergeenko, Z. Phys. C **52**, 635 (1992).
[40] G. I. Lykasov and M. N. Sergeenko, Yad. Fiz. **54**, 1691 (1991) [Sov. J. Nucl. Phys. **54**, 1037 (1991)].
[41] G. I. Lykasov and M. N. Sergeenko, Z. Phys. C **52**, 697 (1992).
[42] G. I. Lykasov and M. N. Sergeenko, Yad. Fiz. **55**, 2502 (1992) [Sov. J. Nucl. Phys. **55**, 1393 (1992)].
[43] G. I. Lykasov and M. N. Sergeenko, Z. Phys. C **58**, 697 (1992).
[44] G. I. Lykasov and M. N. Sergeenko, Yad. Fiz. **59**, 503 (1996) [Sov. J. Nucl. Phys. **59**, 475 (1996)].
[45] G. I. Lykasov and M. N. Sergeenko, Z. Phys. C **70**, 455 (1996).
[46] A. B. Kaidalov, Yad. Fiz. **45**, 1452 (1987) [Sov. J. Nucl. Phys. **45**, 902 (1987)].
[47] R. D. Field and R. P. Feynman, Phys. Rev. D **15**, 2590 (1977); Nucl. Phys. B **136**, 1 (1978).
[48] G. C. Rossi and G. Veneziano, Nucl. Phys. B **123**, 507 (1977).
[49] A. Capella, U. Sukhatme, C. I. Tan, and J. Tran Thanh Van, Phys. Lett. B **81**, 68 (1979).
[50] A. A. Grigoryan, N. Ya. Ivanov, and A. B. Kaĭdalov, Yad. Fiz. **36**, 1490 (1982) [Sov. J. Nucl. Phys. **36**, 867 (1982)].
[51] G. Veneziano, Nuovo Cimento A **57**, 190 (1968).
[52] K. A. Ter-Martirosyan, Phys. Lett. B **44**, 377 (1973).
[53] G. H. Arakelyan, N. Ya. Ivanov, and A. A. Grigoryan, Z. Phys. C **52**, 317 (1991).
[54] M. G. Albrow *et al.*, Nucl. Phys. B **155**, 39 (1979).
[55] M. Schouten *et al.*, Z. Phys. C **90**, 93 (1981).
[56] A. Suzuki *et al.*, Lett. Nuovo Cimento **24**, 449 (1979).
[57] D. Brick *et al.*, Phys. Rev. D **25**, 2248 (1982).
[58] M. Aguilar-Benitez *et al.*, Z. Phys. C **44**, 531 (1989).
[59] N. M. Agababyan *et al.*, Z. Phys. C **46**, 387 (1990).
[60] N. M. Agababyan *et al.*, Z. Phys. C **41**, 539 (1988).
[61] R. Gottgens *et al.*, Z. Phys. C **12**, 323 (1982).
[62] M. Barth *et al.*, Nucl. Phys. B **223**, 296 (1983).
[63] P. V. Chliapnikov *et al.*, Nucl. Phys. B **176**, 303 (1980).
[64] A. Suzuki *et al.*, Nucl. Phys. B **172**, 327 (1980).
[65] S. Frixione, M. L. Mangano, P. Nason, and G. Ridolfi, Nucl. Phys. B **431**, 453 (1994).
[66] S. Brodsky *et al.*, Phys. Rev. D **23**, 2745 (1981).
[67] E. M. Levin, M. G. Ryskin, Yu. M. Shabel'skiĭ, and A. G. Shuvaev, Yad. Fiz. **53**, 1059 (1991) [Sov. J. Nucl. Phys. **53**, 657 (1991)]; Phys. Lett. B **260**, 429 (1991).
[68] P. Nason, S. Dawson, and R. K. Ellis, Nucl. Phys. B **303**, 607 (1988).
[69] W. Beenaker *et al.*, Nucl. Phys. B **351**, 507 (1991).
[70] Particle Data Group, Phys. Rev. D **50**, 1173 (1994).
[71] V. V. Anisovich and V. M. Shekhter, Nucl. Phys. B **55**, 455 (1973).
[72] F. E. Close, *An Introduction to Quarks and Partons* (Academic, New York, 1979).
[73] O. I. Piskounova, Preprint FIAN-140, Lebedev Institute, Moscow (1987).
[74] M. Barlag *et al.*, Phys. Lett. B **247**, 113 (1990).
[75] G. Bari *et al.*, Nuovo Cimento A **104**, 571 (1991).
[76] P. Chavauvat *et al.*, Phys. Lett. B **199**, 304 (1987).
[77] S. Barlag *et al.*, Z. Phys. C **39**, 451 (1988).
[78] M. Aguilar-Benitez *et al.*, Z. Phys. C **31**, 491 (1986).
[79] M. Aguilar-Benitez *et al.*, Phys. Lett. B **161**, 401 (1985).
[80] M. Aguilar-Benitez *et al.*, Phys. Lett. B **169**, 106 (1986).
[81] M. Aguilar-Benitez *et al.*, Phys. Lett. B **201**, 176 (1988).
[82] M. Aguilar-Benitez *et al.*, Z. Phys. C **40**, 321 (1988).
[83] R. Ammar *et al.*, Phys. Lett. B **183**, 110 (1987).
[84] R. Ammar *et al.*, Phys. Rev. Lett. B **61**, 2185 (1988).
[85] M. Aguilar-Benitez *et al.*, Phys. Lett. B **201**, 176 (1988).
[86] R. Werding, in *Proceedings of the Twenty-Seventh Intern. Conference on High Energy Physics*, Glasgow, 1994.
[87] F. Dropmann, in *Proceedings of the Fifth Symposium on Heavy Flavor Physics*, Montreal, 1993.
[88] M. Adamovich *et al.*, Phys. Lett. B **395**, 402 (1993).
[89] G. A. Alves *et al.*, Phys. Rev. Lett. **72**, 812 (1994).
[90] E. M. Aitalia *et al.*, Preprint FERMILAB-Pub-96/001-E, Fermilab, Batavia (1996).
[91] S. J. Brodsky *et al.*, Phys. Lett. B **93**, 451 (1980); R. Vogt and S. J. Brodsky, Nucl. Phys. B **478**, 311 (1996).
[92] O. I. Piskounova, Preprint No. E2-95-275, JINR, Dubna (1995).

[93] G. H. Arakelyan, Preprint Yerphy 1481(18)-96, Yerevan Physics Institute, Yerevan, Armenia (1996).
[94] A. I. Veselov, O. I. Piskounova, and K. A. Ter-Martirosyan, Phys. Lett. B **158**, 175 (1985).
[95] W. Kittel, in *Proceedings of the Twenty-Fourth International Conference on High Energy Physics*, Munich, 1988, p. 625; C. M. J. Lattes, Y. Fujimoto, and S. Hasegawa, Phys. Rep. **65**, 151 (1980).
[96] A. Capella *et al.*, Phys. Lett. B **81**, 68 (1979).
[97] A. Capella, U. Sukhatme, and J. Tran Thanh Van, Z. Phys. C **3**, 329 (1980).
[98] A. Capella and J. Tran Thanh Van, Z. Phys. C **10**, 24 (1981).
[99] P. Aurenche and F. W. Bopp, Z. Phys. C **13**, 205 (1982).
[100] U. Gasparini, in *Proceedings of the Twenty-Fourth International Conference on High Energy Physics*, Munich, 1988, p. 971.
[101] E. L. Berger, in *Proceedings of the Twenty-Fourth International Conference on High Energy Physics*, Munich, 1988, p. 987.
[102] K. Hahn and J. Ranft, Phys. Rev. D **41**, 1463 (1990).
[103] J. Ranft, F. W. Bopp, A. Capella, and J. Tran Thanh Van, Z. Phys. C **51**, 99 (1991).
[104] P. Aurenche *et al.*, Phys. Rev. D **45**, 92 (1992).
[105] V. A. Abramovskiĭ, V. N. Gribov, and O. V. Kancheli, Yad. Fiz. **18**, 595 (1973) [Sov. J. Nucl. Phys. **18**, 308 (1973)].
[106] F. E. Low, Phys. Rev. D **12**, 163 (1975); S. Nussinov, Phys. Rev. Lett. **34**, 1268 (1975).
[107] P. V. Landshoff and O. Nachtmann, Z. Phys. C **35**, 405 (1987).
[108] J. F. Gunion and D. E. Soper, Phys. Rev. D **15**, 2617 (1977); E. M. Levin and M. G. Ryskin, Yad. Fiz. **34**, 1114 (1981) [Sov. J. Nucl. Phys. **34**, 619 (1981)].
[109] J. R. Cudell and D. A. Ross, Nucl. Phys. B **359**, 247 (1991).
[110] J. M. Cornwall, Phys. Rev. D **26**, 1453 (1982).
[111] F. Halzen, G. I. Krein, and A. A. Natale, Phys. Rev. D **47**, 295 (1993).
[112] M. Baker, J. S. Ball, and F. Zachariasen, Nucl. Phys. B **186**, 531, 560 (1981); N. Brown and M. R. Pennington, Phys. Rev. D **38**, 2266 (1988); **39**, 2723 (1989).
[113] C. Bernard, Phys. Lett. B **108**, 431 (1982); J. E. Mandula and O. Ogilvie, Phys. Lett. B **185**, 127 (1987).
[114] A. E. Brenner *et al.*, Phys. Rev. D **26**, 1497 (1982); P. Gapiluppi *et al.*, Nucl. Phys. B **70**, 1 (1974).
[115] F. W. Busser *et al.*, Phys. Lett. B **70**, 471 (1973).
[116] M. N. Sergeenko, Yad. Fiz. **56** (3), 140 (1993) [Phys. At. Nucl. **56**, 365 (1993)].
[117] V. A. Petrov and A. P. Samokhin, Preprint CERN-TH.5583/89, CERN, Geneva (1989); S. J. Brodsky and W.-K. Tang, Phys. Lett. B **318**, 203 (1993).
[118] L. Stodolsky and J. J. Sakurai, Phys. Rev. Lett. **11**, 90 (1963).
[119] A. B. Kaĭdalov and P. E. Volkovitsky, Yad. Fiz. **35**, 1231 (1982) [Sov. J. Nucl. Phys. **35**, 720 (1982)].
[120] A. A. Grigoryan and N. Ya. Ivanov, Yad. Fiz. **43**, 681 (1986) [Sov. J. Nucl. Phys. **43**, 442 (1986)].

Translated by Patricia A. Millard

This article was translated from the preliminary version supplied by the Russian Editorial Office. It differs from the final published version.